Redox Mediators in Homogeneous Co-Electrocatalysis

Amelia G. Reid and Charles W. Machan*

* - machan@virginia.edu; ORCID 0000-0002-5182-1138

A.G.R. ORCID: 0000-0002-2868-4091

Department of Chemistry, University of Virginia, PO Box 400319,

Charlottesville, VA 22904-4319, USA

Abstract

Homogeneous electrocatalysis has been well studied over the last several decades for the conversion of small molecules to useful products for green energy applications or as chemical feedstocks. However, in order for these catalyst systems to be used in industrial applications, their activity and stability must be improved. In naturally occurring enzymes, redox equivalents (electrons, often in a concerted manner with protons) are delivered to enzyme active sites by small molecules known as redox mediators (RMs). Inspired by this, co-electrocatalytic systems with homogeneous catalysts and RMs have been developed for the conversion of alcohols, nitrogen, unsaturated organic substrates, oxygen, and carbon dioxide. In these systems, the RMs have been shown to both increase activity of the catalyst and shift selectivity to more desired products by altering catalytic cycles and/or avoiding high-energy intermediates. However, the area is currently underdeveloped and requires additional fundamental advancements in order to become a more general strategy. Here, we summarize the recent examples of homogeneous coelectrocatalysis and discuss possible future directions for the field.

1. Introduction

Small molecule conversion by homogeneous electrocatalysts is of continuing importance to the mitigation of the problems associated with climate change and increased global energy demand. Reactions such as the alcohol oxidation reaction (AOR),¹ nitrogen reduction reaction (N_2RR) ,² oxygen reduction reaction (ORR),³ and carbon dioxide reduction reaction $(CO_2RR)^4$ all involve the transformation of stable, abundant molecules to value-added chemicals or energy. Homogeneous electrocatalysts are compelling because they are generally active at ambient conditions (standard temperature and pressure) and have well-defined active sites, which make them amenable to mechanistic study and iterative synthetic modification. However, in many reports, these systems require large energy input due to the high overpotentials (η) required to achieve relevant activity. Overpotential is the energy beyond the thermodynamic minimum required to drive an electrochemical reaction at appreciable rates.

1.1. Biological Mediators

In biological systems, nature overcomes significant thermodynamic and kinetic challenges through the use of redox mediators (RMs), which shuttle electron equivalents to active sites where the interconversion of energy and chemical bonds occurs. When the transfer of electrons is accompanied by the transfer of protons these are referred to as electron-proton transfer mediators (EPTMs).^{5, 6} For example, quinones are found in a variety of organisms because of their ability to facilitate reversible proton-dependent redox reactions to and from metallocofactors, which has the added benefit of protecting against the formation of potentially reactive radical intermediates.⁷ During mitochondrial respiration, ubiquinone (UQ) assists in shuttling electrons and protons to several of the active sites in the electron transport chain (Figure 1).8 Many enzymes also rely on iron-sulfur clusters (FeS) distributed throughout their interior matrix to deliver electrons from the surface of the protein structure to a buried active site within the enzyme. 9, 10 These enzymes have evolved so that the energetic difference in oxidation states of each cluster serves as a driving force for electron transfer (ET), harnessing the ability of the cofactors to exist in a variety of redox configurations without having to electronically couple each site directly. 11, 12 This is a requirement because redox-active sites are generally spatially isolated in biological systems and their tertiary structures are static relative to the movement of electrons, protons, and small molecule substrates.

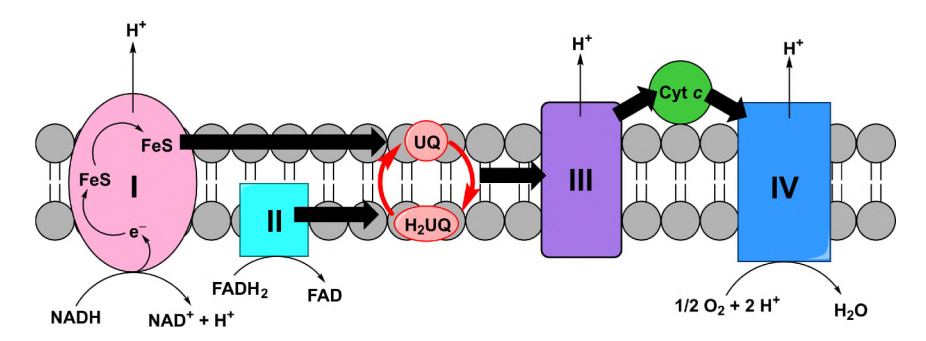


Figure 1. Mitochondrial electron transport chain highlighting redox mediators (1,4-dihydronicotinamide adenine dinucleotide (NADH), flavin adenine dinucleotide (FADH₂), dihydroubiquinone H_2UQ , and iron–sulfur clusters (FeS)) which assist in the reduction of O_2 to H_2O .

1.2. Synthetic Mediators

Inspired by these electron cascades, bioelectrocatalytic systems have been developed that utilize small molecule RMs to deliver electron equivalents to the active sites of enzymes.^{13, 14} Electrochemical glucose sensors that previously relied on the energy-intensive oxidation of hydrogen peroxide (H₂O₂) have been modified to instead use osmium- and ferrocene-based compounds as RMs, which improves their efficiency and stability.^{15, 16} Several other biosensors

that use cytochrome *c* as the mediator have also been developed for the detection of small molecules such as H₂O₂¹⁷ and bilirubin.¹⁸ Fuel cells that rely on co-catalysis with mediators have also been developed for the cathode¹⁹⁻²² or anode²³ as well as for both half-cell reactions.²⁴⁻²⁶ Similar to the way organic molecules have been implemented into biosensors, methyl viologen has been used as a RM with a nitrogenase enzyme catalyst for the reduction of nitrogen to ammonia as the cathodic half-reaction of a hydrogen fuel cell.²⁷ Importantly, in all of these examples, matching the redox potential of the mediator and the enzyme within 50 mV is necessary for optimal efficiency and activity.⁹ This is due to a reliance on outer-sphere ET during the reaction (which necessitates a favorable thermodynamic driving force^{28, 29}) and the need to avoid competing ET pathways which lower selectivity (**Figure 2**). While the addition of RMs into such systems has allowed for increased stability, this type of outer-sphere ET can still react with other small molecules present in the reaction medium¹⁵ leading to long-term instability and inefficiency.

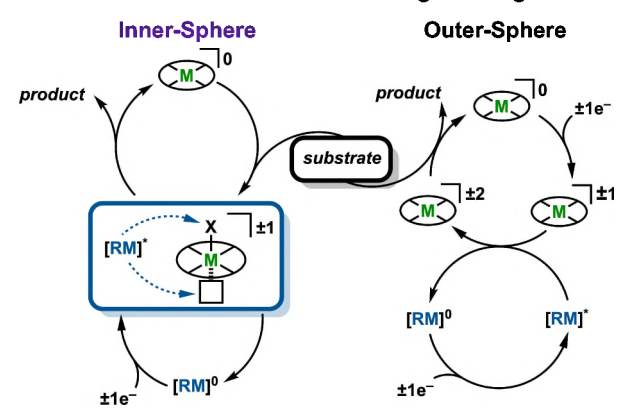


Figure 2. General inner- versus outer-sphere electron transfer mechanisms with a RM, independent of proton transfer, where X = substrate.

The use of RMs, commonly ferrocene (Fc) derivatives, 30-32 has been explored in electrosynthesis, where in contrast to the systems described previously, the RM shuttles electron equivalents in a catalytic fashion via an outer-sphere reaction to transform substrates into reactive intermediates. 33, 34 Other examples use nitroxyl radicals as EPTMs in transformations that rely on a hydrogen atom transfer (HAT) step, where proton and electron movement are directly coupled during direct interaction with the substrate, sometimes when both substrate and EPTM are bound to the same metal center. 35-38 Additionally, RMs have been implemented in photocatalysis to assist in photosensitizer activation 39-44 and in systems for heterogenous CO₂RR to improve activity and selectivity. 45, 46 Although this approach has been recognized as a basic research need for catalysis science, there remains a relatively limited number of homogeneous electrochemical systems with RMs in spite of their potential to improve selectivity, activity and energy efficiency

through thermodynamic and mechanistic analysis.⁴⁷ In this *Perspective*, we discuss examples of RMs in homogeneous co-electrocatalysis, analysis of the key thermodynamic components of these systems, and strategies we believe to be important for further optimization of co-electrocatalytic systems in the future.

2. Recent Examples of Redox Mediators in Homogeneous Co-Electrocatalysis

Despite the limited number of reports involving the use of RMs in homogeneous electrocatalysis, the known systems cover a wide scope of energy-relevant small molecule transformations involving alcohol oxidation (AOR),^{5, 48, 49} dinitrogen reduction (N₂RR),^{50, 51} the hydrogenation of unsaturated organic molecules,⁵² hydrogen oxidation (HOR),⁵³ dioxygen reduction (ORR),^{6, 54, 55} and CO₂ reduction(CO₂RR).⁵⁶⁻⁶⁰ Here, we describe the current known examples of co-electrocatalytic systems where (1) both the catalyst and RM are homogeneous molecular species and (2) at least one of the two is redox-active and regenerated by the electrode. There are additional examples of co-catalytic systems for small molecule transformation that rely on similar properties, but do not meet both sets of criteria and are therefore not discussed in detail in this *Perspective*.^{34, 61, 62} The term 'co-electrocatalytic' is meant to encompass that these transformations are both electrocatalytic and require a co-catalytic component to occur; this description does not require that any individual component is also intrinsically catalytic under the described conditions, although this can be the case.

2.1. Alcohol Oxidation Reaction (AOR)

The first example of co-electrocatalytic AOR is a report by Badalyan and Stahl on the use of 2,2,6,6-tetramethyl-1-piperidine *N*-oxyl (TEMPO) as an EPTM with a (2,2'-bipyridine)Cu(II) triflate catalyst for the AOR (**Figure 3**).⁵ While TEMPO has been widely reported as an electrocatalyst for alcohol oxidation, these systems rely on a H⁺/2e⁻ TEMPO⁺/TEMPOH redox process, which occurs at very oxidizing electrode potentials, making the process relatively energy intensive.⁶³⁻⁶⁷ The co-electrocatalytic system utilizes the lower energy TEMPO/TEMPOH couple to facilitate a HAT reaction when paired with the Cu catalyst, thanks to the activation of the alcohol substrates when coordinated to the Cu metal center. The authors demonstrated that while co-electrocatalysis occurs at the Cu(II/I) redox potential, the nitroxyl radical is necessary for catalysis due to its role as a hydrogen atom acceptor from a Cu(II)-alkoxide intermediate, the formation of which is the rate-limiting step of the reaction.

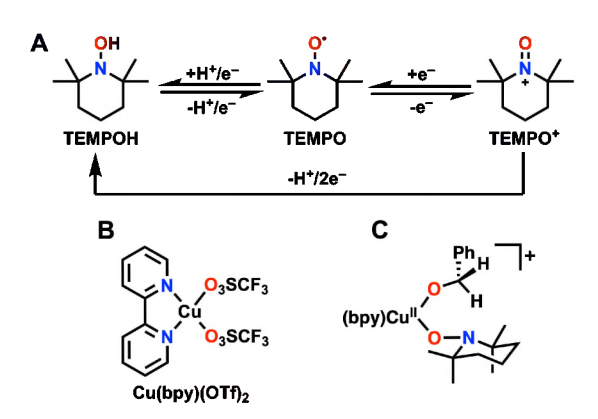


Figure 3. (**A**) Structures from the redox cycle of 2,2,6,6-tetramethyl-1-piperidine *N*-oxyl (TEMPO), (**B**) the Cu(bpy)(OTf)₂ (bpy = 2,2'-bipyridine; OTf = $CF_3SO_3^-$) complex, and (C) the intermediate species formed following the rate-limiting deprotonation of the alcohol substrate (benzyl alcohol in this example) in Ref ⁵.

The Waymouth Group has published two co-electrocatalytic systems for the AOR, the first of which by Galvin and Waymouth uses an Ir(PNP)(H)₂ complex, where PNP is bis[2diisopropylphosphino)ethyl]amide, (Figure 4) with several electron-rich phenol derivatives as the EPTM. 48 The authors rationalized that activity for the AORs of interest could be achieved at lower overpotentials by eliminating the need to directly oxidize relatively stable metal-hydride (M-H) species, since the energy-intensive oxidative deprotonation of these intermediates is generally the limiting kinetic step of the intrinsic catalytic cycle. They found that the addition of a phenol derivative to a solution containing the Ir(PNP)(H)₂ pincer catalyst led to a significant shift in oxidation potential to much lower energy (more negative potential for the oxidation event which initiates catalysis) due to the interception of the M-H intermediate. The proposed catalytic cycle depends on a HAT step, where a phenoxyl radical accepts a hydrogen atom from the M-H. In total, two successive HAT steps are necessary to complete the catalytic cycle, each of which could represent the rate-determining step (RDS) of the reaction (Figure 4). By examining a series of phenol-based molecules as the EPTM, Galvin and Waymouth were able to demonstrate that as the pK_a of the phenol becomes more acidic, the observed oxidation potential of the corresponding phenoxide decreases (shifts to more negative potentials) in a manner that can be used to tune the operating potential of the co-catalytic system.

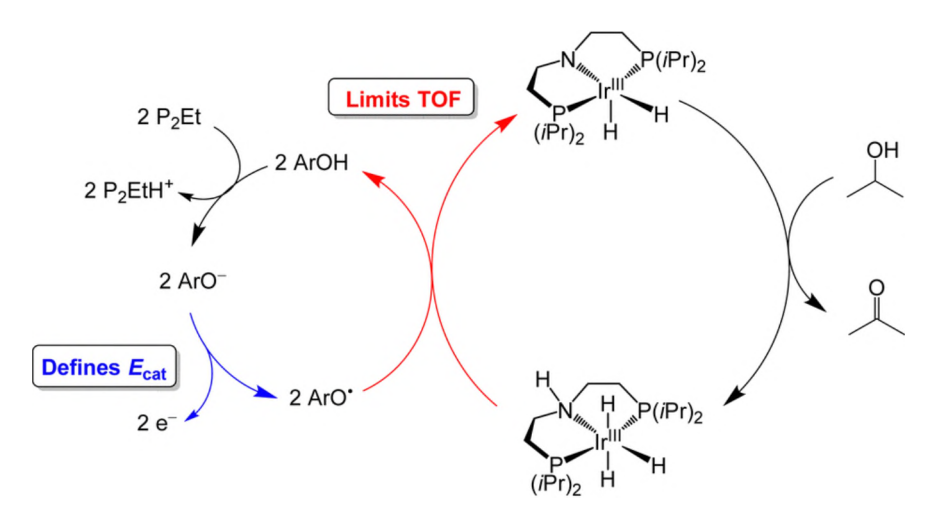


Figure 4. The proposed catalytic cycle for oxidation of 2-propanol by Ir(PNP)(H)₂, where PNP is bis[2-diisopropylphosphino)ethyl]amide, in the presence of the phenoxyl radical mediator. Reproduced from Ref. 68 with permission from the Royal Society of Chemistry.

Shortly following this report, McLoughlin et al. disclosed a second co-catalytic system for the AOR using an efficient Ru-based ketone transfer hydrogenation catalyst and a Ru-centered EPTM, **Ru^{III}N** (**Figure 5**). ⁴⁹ Under thermal catalytic conditions, the catalyst can oxidize isopropanol to acetone in order to drive the reduction of ketone substrates, generating a Ru(II) hydride intermediate **RuH**. They found that the electrocatalytic oxidation of isopropanol could be achieved if an electrode poised at suitably oxidizing potentials was substituted for the ketone substrate, ⁶⁹ noting that the two-electron, one-proton oxidation of the intermediate Ru(II) hydride complex RuH was likely to be the rate-determining step of the catalytic cycle. Subsequently, inspired by previous work, 5, 38 McLoughlin et al. reasoned that the introduction of a suitable hydrogen atom acceptor could again access an appreciable catalytic response at less oxidizing potentials (lower overpotentials) by circumventing the stepwise removal of a proton and electron during the oxidation of the key metal hydride intermediate. 49 In order to implement this strategy, the authors developed a set of guidelines for the selection of an EPTM with the appropriate thermodynamic properties: (1) the BDFE of the relevant M-H intermediate must be similar to that of the EPTM-H bond, (2) the $E_{1/2}$ and p K_a of the EPTM must be close to the thermodynamic potential for the AOR, (3) the EPTM must be oxidized at more negative potentials than the targeted M-H intermediate, and (4) the p K_a of the EPTM-H should be in the range where the hydrogen evolution reaction (HER) is unfavorable. The system functioned as intended, lowering the overpotential for isopropanol oxidation by ca. 450 mV, in spite of the limited knowledge of relevant thermodynamic parameters in the THF operating solvent, which precluded definitive thermodynamic positioning of several reaction steps. Additionally, high Faradaic efficiency of the desired product was maintained with minimal HER observed.

Figure 5. Co-electrocatalytic cycle proposed by McLoughlin *et al.* for isopropanol (iPrOH) oxidation by a Ru-centered transfer hydrogenation catalyst paired with a metal-based HAT acceptor Ru^{III}N. Following HAT between RuH and Ru^{III}N, the resulting Ru^I and Ru^{III}NH products can be regenerated by the electrode to close the cycle.

2.2. Nitrogen Reduction Reaction (N₂RR)

Leveraging extensive work on the reduction of N_2 with chemical reducing agents by the Peters group^{70, 71} Chalkley *et. al* were able to develop a homogeneous co-catalytic system with a Cobased EPTM for N_2 RR in 2018.⁵⁰ Previously, in 2017 Chalkley *et al.* reported that $P_3^BFe^+$, where $P_3^B = tris(o$ -diisopropylphosphinophenyl)borane, was a competent catalyst for the reduction of N_2 to ammonia (N_3) with dihydrogen as a co-product when cobaltocene (Cp^*_2Co) was used as the chemical reductant in the presence of acid.⁷² In the subsequent 2018 report, it was established that the Cp^*_2Co EPTM could be electrochemically recycled during co-electrocatalytic N_2RR with $P_3^BFe^+$.⁵⁰ The authors discovered that the rate of catalysis was dependent on the pK_a of the acid used because the protonation of the EPTM to form $Cp^*(\eta^4-C_5Me_5H)-Co^+$ was essential to the coelectrocatalytic cycle. This activated cationic Co-based EPTM was proposed to possess C–H bonds weak enough to position it as a proton-coupled electron transfer (PCET) reagent capable of generating N_-H bonds during catalysis (**Figure 6**). A more recent study of this EPTM by the same group shows the generality of this approach to co-electrocatalytic systems by substituting the Fe-based catalyst for other transition metals that bind N_2 . This report establishes the excellent

generality of this approach, as all systems function co-electrocatalytically, however, competitive HER is observed in all cases.⁵¹

Figure 6. Calculated thermodynamics and kinetics of synchronous PCET and asynchronous PCET (PT–ET) between P_3^B FeNNH and $[Cp^*(exo-\eta^4-C_5Me_5H)Co][OTf]$ to generate P_3^B FeNNH₂. Note: k_{rel} for ET is defined as 1 M⁻¹ s⁻¹. Reprinted with permission from *J. Am. Chem. Soc.* **2018**, 140, 6122–6129. Copyright 2018 American Chemical Society.

2.3. <u>Hydrogenation of Unsaturated Substrates</u>

The electrocatalytic hydrogenation of unsaturated organic molecules can proceed via a M-H intermediate, however, at reducing potentials these intermediates can also rapidly be reduced again to lead to competitive HER. However, a recent study by Derosa et al. exploits the use of the same class of Co-based EPTM described in Section 2.2 to circumvent this issue by forming a M-H intermediate at more positive potentials than those required for HER.⁵² To achieve this, Ni-centered catalyst, [P4^{Me}Ni^{II}]²⁺, was paired [CpCoCp^{NMe2}]⁺ as an EPTM (Figure 7). For this Nibased catalyst, the two-electron reduction potential of Ni^{II} to Ni⁰ generates a species which can be protonated by an acid of sufficient strength to form a readily reduced Ni^{II}-H. This means that at a comparable potential to the Ni^{II}/Ni⁰ reduction, the reduction of Ni^{II}–H to Ni^I–H can occur, which initiates HER in the presence of the external acid. However, at potentials which are more positive than those required for Ni^{II}/Ni⁰ and Ni^{II}–H/Ni^I–H reduction, the Co-based EPTM is protonated and reduced to generate its activated form, [CpCoCpNHMe2]+, which can transfer a hydrogen atom equivalent via a PCET step to $[P_4^{Me}Ni^{II}]^{2+}$, forming $[P_4^{Me}Ni^{III}-H]^{2+}$. At the potentials required for the reduction of the Co-based RM, this Ni^{III}–H hydride species is rapidly reduced to a Ni^{II}–H, but these potentials are not reducing enough to complete the Ni^{II}-H/Ni^I-H reduction. The result is that the intermediate compound Ni^{II}-H is available and capable of hydride transfer to unsaturated substrates like methyl phenylpropiolate under conditions which limit competitive HER. Like the examples for the N₂RR discussed above, all of the systems tested showed some competitive HER even at the less reducing potentials, which is likely a consequence of the presence of multiple species with BDFEs weaker than H₂, *vide infra*.

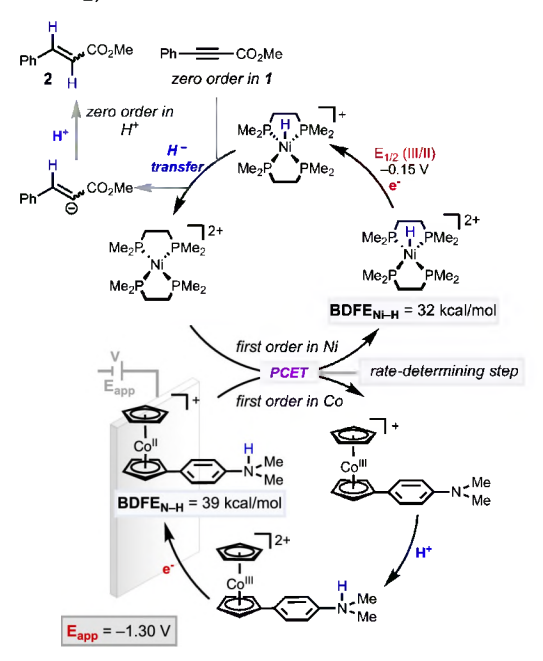


Figure 7. Plausible mechanistic pathway accounting for the tandem reductive electrocatalysis discussed herein, consistent with the data described in the text. Reprinted with permission from *J. Am. Chem. Soc.* **2022**, *144*, 20118-20125. Copyright 2022 American Chemical Society.

2.4. Hydrogen Oxidation Reaction (HOR)

The only example reported for the HOR involves the use of an Fe-centered catalyst, [Fe(PEtNPhPEt)-(CO)3]*, where PEtNPhPEt is (Et2PCH2)2NMe, and a Cr-based EPTM.⁵³ The Cr-centered EPTM exists in an equilibrium between its dimeric form, [Cp*Cr(CO)3]2, and a 17-electron species, Cp*Cr(CO)3. The slowest reaction step in the co-electrocatalytic cycle is the homolytic activation of H2 by two equivalents of Cp*Cr(CO)3 to generate an intermediate chromium hydride in a purely thermal step. The resultant Cp*Cr(CO)3H complex can transfer a hydrogen atom equivalent to the monocationic [Fe(PEtNPhPEt)-(CO)3]* to form an [Fe-H]* which can quickly be deprotonated by added base to generate a formally Fe(0) species. The formally Fe(0) species is oxidized at the electrode to close the cycle, regenerating all components and dictating the required operating potential. Analysis of the reaction components revealed that the chosen base, 2-methylpyridine, was not basic enough to deprotonate the chromium hydride. Further, control testing showed that the oxidation of Cp*Cr(CO)3 and Cp*Cr(CO)3H occurred at potentials more positive than that of the [Fe(PEtNPhPEt)-(CO)3]* redox event which initiated coelectrocatalysis, meaning that no electrochemical activation of the Cr species occurs as a part of the reaction cycle. Although no BDFEs were reported for any of the hydride species proposed,

the observation of facile hydrogen atom transfer from Cr to Fe suggests that this reaction could be favored thermodynamically.

2.5. Oxygen Reduction Reaction (ORR)

Anson and Stahl published a study on Co(salophen) as the catalyst for the ORR with *p*-benzoquinone (BQ) as an EPTM (**Figure 8**).⁶ This study was a follow-up to an earlier study on the mechanism of Co(salophen)-catalyzed oxidation of *p*-hydroquinone (the reduced form of BQ) under aerobic conditions.⁷³ In contrast to the intrinsic inactivity of some of the catalysts in the AOR system discussed above, the Co(salophen) metal complex catalyzes the ORR in the absence of the EPTM, producing hydrogen peroxide (H₂O₂; the 2e⁻/2H⁺ product). However, when *p*-hydroquinone is present, the system selectivity shifts from H₂O₂ to water (H₂O; the 4e⁻/4H⁺ product) and an increase in rate is observed. Both changes are explained by the authors' proposed mechanism: a Co(III)-superoxide intermediate reacts initially with H₂Q via HAT, which is followed by a PCET step that leads to the formation of water. This pathway for water formation avoids the production of H₂O₂, an undesirable product in polymer electrolyte membrane fuel cells,⁷⁴ while also increasing the rate of the ORR. The authors also found that using an EPTM with a more positive reduction potential, 2-chlorohydroquinone (2-CIH₂Q), increased the rates of catalysis relative to BQ used at the same more positive potential.

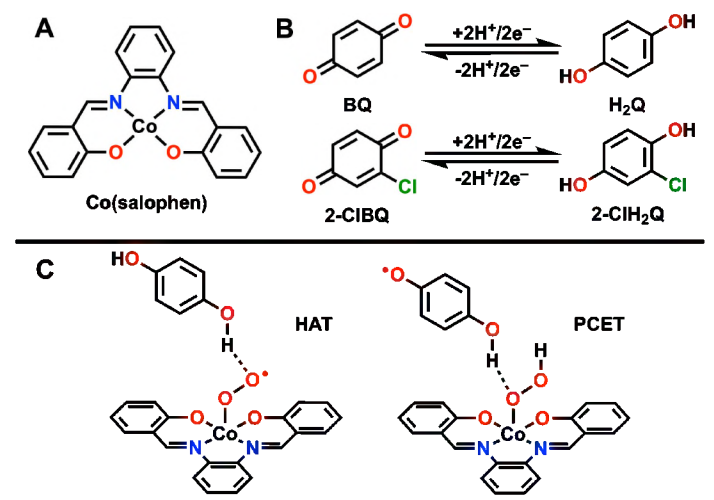


Figure 8. The structures of the Co(salophen) catalyst (A) and p-hydroquinone (H₂Q) and 2-chlorohydroquinone (2-ClH₂Q) EPTMs (B) from Ref ⁶. The relevant hydrogen atom transfer (HAT) and proton-coupled electron transfer (PCET) steps proposed in the reduction of the Co(III) superoxide intermediate.

Inspired by the work of Anson and Stahl,⁶ our lab has also studied the use of benzoquinone (BQ) as an EPTM with a Mn-centered catalyst, Mn(^{tbu}dhbpy)Cl where (^{tbu}dhbpy)(H)₂ is 6,6'-di(3,5-di-*tert*-butyl-2-hydroxybenzene)-2,2'-bipyridine (**Figure 9**).⁵⁴ In this example, a change in the

intrinsic selectivity of the catalyst for H₂O₂^{75, 76} to favor H₂O is observed when BQ and 2,2,2trifluoroethanol (TFEOH) are present in solution. BQ is typically reduced by two electrons in a stepwise fashion under aprotic conditions in non-aqueous solvents, but in the presence of TFEOH the reduced species are stabilized by hydrogen bonding-interactions, shifting to a two-electron reduction as the reduction potential of the second electron shifts to more positive potentials than the first reduction (potential inversion). In the co-catalytic system with Co(salophen), Anson and Stahl used AcOH as the proton donor, which is strong enough to fully protonate the benzoquinone dianion under standard thermodynamic conditions; under our chosen reaction conditions, TFEOH should only monoprotonate the same dianion.⁷⁷⁻⁸⁶ However, at high proton donor concentrations, the solvent mixture becomes non-ideal, as a cluster of proton donors forms around the initially favored monoprotonated species, which was assessed by electrochemical means to have an approximate formulation of [HQ(TFEOH)₄(TFEO)₁]^{2-,78,87,88} In this non-covalent assembly, it is possible to form a hydrogen bond-stabilized H₂Q species, [H₂Q(TFEOH)₃(TFEO)₂]²⁻ that functions as an EPTM to a Mn(III) superoxide intermediate, intercepting the intrinsic catalytic mechanism and shifting product selectivity from H₂O₂ to H₂O. We found that although this electrogenerated non-covalent EPTM assembly is more reactive⁸⁹ than p-hydroguinone generated under the conditions reported by Anson and Stahl with a much stronger acid, 6 its co-catalytic function was the same, resulting in a shift in product selectivity from H₂O₂ to H₂O and an increase in the observed activity. Under our reported co-electrocatalytic conditions⁵⁴ we proposed that the consumption of the reduced EPTM results in the delivery of one proton and two electrons overall, accompanied by the release of additional proton donors to complete the reaction: the strong association of 2,2,2-trifluoroethanol in the cluster will weaken rapidly as the hydrogen bondstabilized *p*-hydroquinone cluster is oxidized.

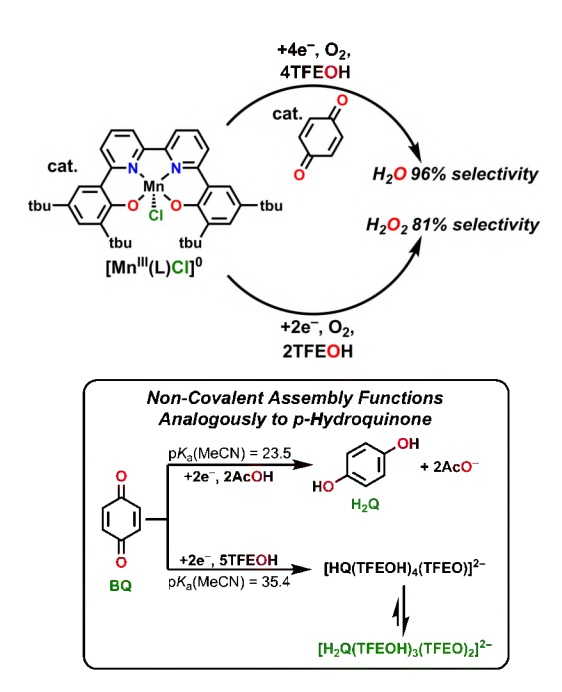


Figure 9. Structure of Mn(tbudhbpy)Cl catalyst developed in our lab where (tbudhbpy)(H)₂ is 6,6'-di(3,5-di-*tert*-butyl-2-hydroxybenzene)-2,2'-bipyridine and summary of results in Ref 54. Reproduced from Ref. 90 with permission from the Royal Society of Chemistry.

A co-electrocatalytic system for the ORR that does not contain a transition metal-centered catalyst or RM was published by Gerken and Stahl based on the combination of the nitroxyl mediator TEMPO and NO_x species.⁵⁵ Nitric oxide (NO) can react with half an equivalent of dioxygen to form nitrogen dioxide (NO₂) in a reaction that is both thermodynamically favorable and kinetically facile. TEMPO, when added to the system, is oxidized by NO₂ in the presence of trifluoroacetic acid to give an equivalent of H₂O, while generating TEMPO⁺ and nitrite (NO₂⁻) as co-products. Based on literature precedent, under the protic reaction conditions NO₂⁻ is thought to be protonated twice to release water with the formation of N₂O₃, which can dissociate to regenerate NO and NO₂. TEMPO⁺ is then reduced at the electrode to close the co-electrocatalytic cycle. Interestingly, although it is possible for TEMPOH (which can also be oxidized by NO₂) to form in solution via the acid-assisted disproportionation of TEMPO, the primary implied redox cycling is TEMPO^{+/0}, meaning that TEMPO is proposed to function primarily as a RM and not as an EPTM. As has been the case with several examples discussed above, neither component is a competent ORR catalyst individually, but the combination of the two components takes advantage of facile and thermodynamically favorable reactivity to mediate the reaction at much more positive potentials than is possible with homogeneous transition metal-based catalysts. The authors went on to demonstrate the generality of this approach by achieving co-electrocatalysis with 4-acetamidoTEMPO (ACT), 3-carbamoyl-2,2,5,5-tetramethyl-1-pyrrolidinyl-N-oxyl (3CARP), and 9-azabicyclo[3.3.1]nonane-N-oxyl (ABNO). Although all systems showed good stability and activity for ORR, under the electrochemical conditions tested the system was limited by the loss of NO_x species to the gaseous headspace of the cell.

2.6. Carbon Dioxide Reduction Reaction (CO₂RR)

Inspired by biological systems, which accumulate and distribute protons and electrons to metallocofactors during catalysis, Smith *et al.* reported the first example of an EPTM for homogeneous co-electrocatalysis for the CO₂RR in 2019 using the well-studied iron tetraphenylporphyrin ([Fe(TPP)]⁺) catalyst with a series of nicotinamide adenine dinucleotide (NADH) analogues as the EPTM. (**Figure 10**).⁵⁶ Consistent with a co-electrocatalytic response, the addition of the EPTM leads to a greater catalytic rate for the optimized co-catalytic system than the intrinsic activity of [Fe(TPP)]⁺ (13-fold increase) under the same conditions. This system does not see a change in selectivity when the EPTM is added; the exclusive CO₂ reduction product remains carbon monoxide (CO). The series of EPTMs that were tested by the authors allowed them to identify two trends for EPTM selection: (1) the EPTM must be capable of mediating the transfer of both protons and electrons and (2) the closer the reduction potential of the EPTM and catalyst are to one another, the more of an activity enhancement during coelectrocatalysis.

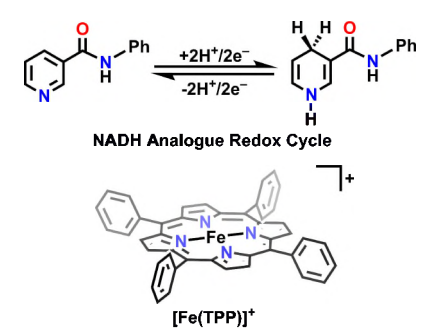


Figure 10. The structures of the iron tetraphenylporphyrin ([Fe(TPP)]⁺) catalyst and RM with the highest activity for the CO₂RR in Ref ⁵⁶.

Further, this study by Smith *et al.* showed through testing with control compounds that while both electron transfer and proton transfer were implicated, when combined in the same EPTM the enhancement effect was greater than the sum, suggesting a more complex mechanism. This point is important, since it had been established previously^{91,92} that the inclusion of hydrogen bond donors in solution has a positive effect on CO₂RR. Mechanistic experiments suggested that the pyridine-based EPTMs were reduced by an *ECEC* mechanism (where *E* and *C* are electron transfer and chemical reaction steps, respectively), with potential inversion for the second reduction event favored at high concentrations of proton donor: at high proton donor

concentrations the species formed after the initial reduction and protonation is more easily reduced than the starting pyridine species. Although this potential inversion by definition establishes the thermodynamic conditions required for a disproportionation reaction to be viable (EPTM(I)+EPTM(I))+EPTM(I)+EPTM(I)), 93 additional control compounds suggested that radical mechanisms were unlikely to assist in catalysis. This is an important point because radical nicotamides have much lower BDFE values than the fully reduced compounds 94 and could potentially react as HAT reagents. Thus, the results of Smith *et al.* imply the possibility of a two-electron redox event, accompanied by one or two protons in a concerted way.

More recently, Mougel et al. reported a system for the reduction of CO_2 to formic acid (HCOOH) using Mn(bpy)(CO)₃Br^{95, 96} and an FeS cluster as an EPTM.⁶⁰ Interestingly, this system also employs a HAT step in the reaction mechanism to avoid inefficient stepwise electron and proton transfer steps, but in this case the authors sought the formation of a M–H species. Therefore, the BDFE of the EPTM–H and M–H species, as well as the pK_3 of the acid used, were important thermodynamic values to consider. Similar to other studies discussed here, the authors were able to alter reaction selectivity and the rate of product formation when using the EPTM in comparison to the intrinsic catalytic properties of the Mn-based complex. In this case, the Mn-centered catalyst is selective for CO under electrochemical conditions, ⁹⁶ but in the presence of the FeS cluster EPTM, the selectivity shifts to HCOOH. This is due to the EPTM promoting the formation of Mn¹(bpy)–H at more positive potentials than [Mn⁰(bpy⁻)]⁻ forms, the latter species being the initial step of the electrocatalytic reduction of CO₂ to the alternative CO product (**Figure 11**).⁴

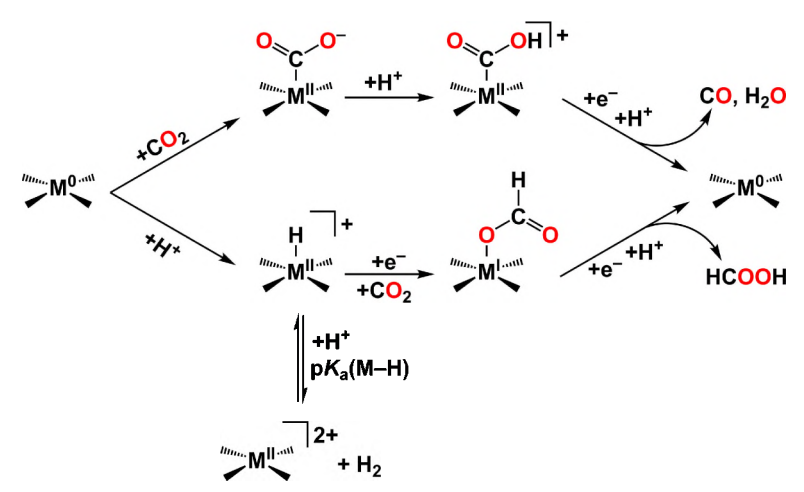


Figure 11. The two most common 2e⁻/2H⁺ pathways for the CO₂RR which determine selectivity between carbon monoxide (CO) and formic acid (HCOOH) and competitive HER pathway.

Motivated by the elegant examples discussed above, we have been investigating small molecules with reduction potentials near the catalytic potential of a Cr catalyst developed in our group. 97, 98 Our initial studies focused on RMs with more negative reduction potentials than the Cr catalyst under the basic premise that to drive electron transfer during CO₂RR, downhill reactions would offer the most benefit. During our screening process we observed that the greatest current enhancement of Cr(tbudhbpy)(H2O)Cl (Figure 12A) arose with sulfone-based RMs (Figure 12B and 12C). It should be emphasized that the role of the sulfone is to shuttle electron equivalents only and does not involve an associated proton transfer, functioning as an RM instead of an EPTM. We initially identified the ability of the Cr-catalyst to catalyze the reduction of CO2 with dibenzothiophene 5,5-dioxide (DBTD) as a RM.^{57, 58} The combination of Cr(^{tbu}dhbpy)(H₂O)Cl and DBTD catalyzes the reductive disproportionation of CO₂ to CO and carbonate (CO₃²⁻) under aprotic conditions. Since the ability to catalyze the reduction of CO₂ under aprotic conditions is not inherent to either the catalyst or RM, we concluded that the electron transfer was occurring via an inner-sphere pathway where the reduced RM binds to Cr during the catalytic cycle in order for the electron transfer from the RM to catalyst to occur. DFT calculations indicated that Crsulfone bond formation, dispersion effects, and through-space conjugation (TSEC)⁹⁹ between the bpy-backbone of the ligand and DBTD stabilized the key intermediate prior to the rate-determining step. In TSEC, a single electron is shared between two π systems of appropriate symmetry and orientation (Figure 13).99 Although an increase in activity also occurred under protic conditions when Cr(tbudhbpy)(H2O)Cl and DBTD were combined, we were unable to exclude the possibility that the reduced DBTD RM acted as an outer-sphere electron transfer reagent, since it was reduced at potentials negative of where the Cr-based complex displayed intrinsic CO₂RR activity.

Figure 12. The structures of both Cr-based catalysts and RMs from Refs. 57 and 59.

This is in contrast to the work by Smith *et al.* where the greatest increase in co-catalytic activity is observed when the EPTM is reduced at a potential slightly positive of the catalyst. We attribute this difference in potential requirements to the large difference in the upper-limit turnover frequency (TOF_{MAX}) values of $[Fe(TPP)]^+$ in comparison to our $Cr(N_2O_2)$ catalyst. Given the significant intrinsic activity of $[Fe(TPP)]^+$, the mediator must be in an activated form prior to potentials where the unimolecular catalytic cycle occurs, such that the co-elecytrocatalytic cycle is competitive with the intrinsic one. The comparatively lower intrinsic activity of our $Cr(N_2O_2)$ catalyst allows the co-electrocatalytic pathway to be competitive, even though it is accessed at more negative potentials than those required to produce a catalytically competent Cr species.

In the initial co-electrocatalytic studies, we proposed that the protic mechanism relied on pancake bonding (PB), where π systems share two electrons that are antiferromagnetically paired (Figure 13). Since it is known that PB can be improved by synthetically increasing the delocalization of the participating radical as well as increasing steric protection, 100-103 we examined protic reaction conditions with a new Cr-based complex and three additional sulfone-containing RMs which varied in their steric properties and electronic structure (Figure 12).⁵⁹ Our results demonstrated that an inner-sphere electron transfer mechanism stabilized by PB between the bpy backbone of the ligand and the RMs could become the dominant pathway under protic conditions, if the interaction between the two components was favorable enough.⁵⁹ It is worth emphasizing that since all of the RMs in this study are reduced at more negative potentials than the catalyst, co-electrocatalytic reduction of CO₂ is initiated at the $E_{1/2}$ of the RM. When comparing the activity of the systems across the series, we found that the RMs with more positive reduction potentials, closer to the reduction potential of the catalyst, had the highest co-electrocatalytic rates. Computational studies showed that the barrier for the rate-determining transition state, cleavage of the C-OH bond in a [RM-Cr-CO₂H]²⁻ adduct, was uniformly lower for all RM derivatives than the intrinsic catalytic cycle of the Cr complexes. However, it was determined that the favorability of adduct formation increased as the standard reduction potential of the RM became more positive, meaning that catalytic rates scaled inversely with the catalytic potential. This sulfone-based RM system is the only example presented in this *Perspective* that is proposed to rely on an inner-sphere electron transfer mechanism sensu stricto, where a RM binds to the metal center and an electron is directly transferred between the two to initiate the subsequent cocatalytic pathway to be accessible.

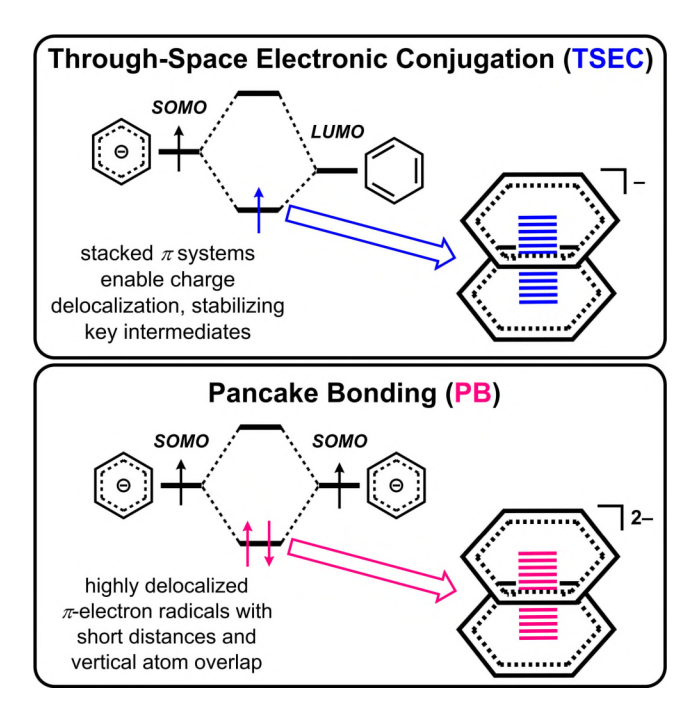


Figure 13. Possible stabilizing forces for key intermediates in the proposed inner-sphere cocatalytic mechanisms described in Refs. ⁵⁷ and ⁵⁹. Adapted from Ref. 59 with permission from the Royal Society of Chemistry.

3. Critical Analysis of Homogeneous Redox Mediator Development

Based on these examples, we can highlight key observations and preliminary conclusions about desirable properties for RMs in molecular co-catalytic systems. Much like the use of thermodynamic positioning in natural systems to establish energy gradients, electron transfer events (with or without a proton) in artificial systems rely on reactions which are at least isoergic, but preferably exergonic in the forward direction. It should be emphasized that while the primary function of a *catalyst* is not to create favorable thermodynamics for catalytic reactions, but rather to render them kinetically accessible, the thermodynamic positioning of all elementary reaction steps can impact speciation relevant to the catalytic process and consequently the observed activity. Therefore, the key challenge to developing a co-catalytic system is to critically assess how the slowest and least efficient steps of the system can be supplanted with alternative routes.

The distinct advantage of the co-catalytic approach is the ability to *independently* select the properties of the secondary component without synthetically modifying the catalyst of interest. In single-component electrocatalysts, modification of the ligand framework to include electron-donating or electron-withdrawing functional groups will impact the standard reduction potential of

the catalytic center. To a first approximation, the standard potential of a catalytic center can be linked to the observed activity in a basic linear free energy relationship, since the thermodynamic positioning of intermediates and kinetic barriers of interest can depend on the same intrinsic properties that dictate reduction potential. The caveat to this generalization is that this type of 'scaling relationship' can only rigorously occur within a catalyst 'family' where the mechanism remains consistent. Several synthetic strategies for circumventing this link between standard reduction potential and activity have been developed, the majority of which rely on manipulating secondary-sphere effects based on positioning charge and hydrogen-bond donors. A strategy for improving the activity and selectivity of a catalytic system that does not require systematic synthetic modifications of the ligand framework is relatively attractive in terms of time and cost.

As a predictive tool, the Bordwell equation has been used to determine X–H bond strengths via a thermodynamic scheme that uses acid strength and standard reduction potential, 109 most commonly in combination with a solvent-dependent correction for the one-electron reduction potential of H⁺. ¹¹⁰ Initially, Bordwell *et al.* used the data from the solution-phase thermochemical cycle to estimate bond dissociation enthalpies (BDEs), 110 however, since this initial implementation it is more common to determine bond dissociation free energies (BDFEs) from these data. BDEs correspond to the enthalpy associated with homolytic bond cleavage in the gas phase, whereas BDFEs incorporate the effects of solvation relevant to homogeneous reactions, including enthalpic and entropic components. Where possible, we have tried to use BDFE values to describe our analysis of the reaction chemistry, although it is important to note that these are not always available. We also note that the Mayer group has recently proposed to re-calibrate these values by referencing PCET potentials against the standard potential of the 2H⁺/H₂ couple in the solvent of interest. 94, 111 For PCET redox couples with an equivalent number of proton and electron transfers, they argue that the use of the potential for H₂ gas formation as the reference state can produce a value which is largely independent from solvent and solution conditions and can even be conceptually described as the free energy of hydrogenation, which has significant utility in the context of thermochemical cycles. Lastly, for multisite-PCET reactions where the electrons and protons are not spatially co-located at some point in the reaction coordinate, the Bordwell equation can also be used to determine an 'effective' BDFE value. 112

3.1. Requirements for Relative EPTM X-H Bond Strength in Co-Electrocatalysis

Independent of the preferred thermodynamic reference state, the known examples of coelectrocatalysis generally leverage the generation of relatively weak sacrificial X–H bonds for reductive processes (such that the desired product bond is stronger) and comparatively strong ones relative to the substrate bond of interest for oxidative processes. In the pioneering example by Badalyan and Stahl,⁵ TEMPO'/TEMPOH cycling (BDFE 66 kcal/mol in MeCN⁹⁴) during the oxidative conversion of alcohols to aldehydes only becomes feasible upon the inclusion of a Cu complex as co-catalyst. As described above, mechanistic studies showed that deprotonation of the Cu(II)-coordinated alcohol is rate-limiting under optimized catalytic conditions, prior to a net hydride transfer (H⁺/2e⁻) from the resultant Cu(II) alkoxide. As a representative example, we shall consider the MeOH oxidation activity reported for this co-electrocatalytic system. The BDFE of the O–H moiety in MeOH has been estimated to be 96.4 kcal/mol⁹⁴ and the expected weakening induced by coordination¹¹³ does not appear to be sufficient to generate net hydrogen atom donation to [TEMPO']. By comparison, the known C–H BDEs of MeOH¹¹⁴ are weaker (96.1 ± 0.2 kcal/mol) than the O–H BDE (104.6 ± 0.7 kcal/mol). However, for the reaction to proceed an intermediate Cu(II) methoxide species should experience the net loss of H⁺/2e⁻ to generate formaldehyde under these conditions. Based on the applied potential, Badalyan and Stahl excluded a two-electron, one-proton TEMPO⁺/TEMPOH-based reaction cycle, which is catalytically competent at more oxidizing potentials.

Prior computational studies on the aerobic system by Ryland et al. suggested that the mechanism proceeded via a six-membered transition state involving an O-coordinated TEMPO leading to a Cu(I)-coordinated [R₂N(H)O] intermediate (**Figure 14**). This [R₂N(H)O] species is a valence tautomer of TEMPOH which rearranges to the latter as part of a thermodynamically favorable net dissociation reaction. 115 Since the formation of Cu¹ and TEMPOH is proposed to be thermodynamically favorable, the C-H substrate bond must be weakened through coordination, given the significant thermodynamic differences described above. We speculate here that the viability of this co-catalytic system at the Cu(II)/Cu(I) redox potential could then imply the existence of a redox equilibrium being established between formally [Cu(II)(OMe⁻)]⁺ and [Cu(I)(OMe')] configurations. Equilibrium electron transfer involving the Cu center would weaken the C-H bonds of the methoxide, rendering the net transfer of a proton and an electron to the cocatalyst TEMPO' more thermodynamically viable. Thus, the favorable driving force of each step would be consistent with the authors' proposal of net hydride abstraction from the intermediate Cu(II) methoxide being distributed as an electron to the Cu(II) center and a proton and electron to [TEMPO].⁵ This mechanistic interpretation is based on the thermodynamic inaccessibility of [TEMPO] and [TEMPOH] under reaction conditions as established by the authors, in conjunction with the low bond BDE of 21.1 kcal/mol estimated for [H–CH₂O^{*}]. This analysis also reconciles with the observation that thermodynamic driving force is almost always a primary determinant in HAT reactivity. 117 An alternative way to consider an inner-sphere redox continuum in this context is as a spin polarization effect on the alkoxide when coordinated to the d^9 Cu(II) center that makes net HAT from $[Cu(II)(OMe^-)]^+$ to coordinated TEMPO* feasible when coupled with Cu(II) reduction.^{117, 118}

$$(bpy)Cu^{\parallel} \xrightarrow{O-N} + (bpy)Cu^{\parallel} + (bpy)Cu$$

Figure 14. Mechanism for aerobic alcohol oxidation by the Cu(bpy)/TEMPO system proposed from hybrid functional DFT methods by Ryland *et al.* in Ref. 115 NMI = N-methylimidazole; S = acetonitrile; R₁ = H, alkyl, aryl; R₂ =alkyl, aryl.

Aerobic oxidation reactions like the Cu/TEMPO system can be an entry point to co-catalytic systems since they generally involve electron and proton transfer to a substrate via a mediator, which is recycled by O₂ during the reaction. The Co(salophen)/p-hydroquinone demonstrated by Anson and Stahl is an alternative version of this, where a co-electrocatalytic system for the ORR can be achieved when an electrode serves as the source of electrons instead of oxidizable substrates.⁶ Although HAT involving the EPTM was shown to play a role in the mechanism of ORR (Figure 8), the role of O-H BDFE in the reaction was not directly examined. While 2-chlorop-benzoquinone was tested for comparison with p-hydroquinone as an EPTM, the computationally estimated BDFE of its O-H bond in DMSO of 84.7 kcal/mol is comparable to that of 83.4 kcal/mol predicted for p-hydroquinone at the same level of theory. 119 Although the use of 2-chloro-p-benzoquinone results in greater rates of catalysis at more positive potentials than pbenzoquinone, as the authors point out this is likely due to the ability to generate greater amounts of 2-chloro-p-hydroquinone relative to p-hydroquinone at the chosen operating potential.⁶ Thus, it is the relative concentration of the activated mediator which results in an increased catalytic response, instead of a difference in BDFE. However, the known role of HAT in the coelectrocatalytic activity implies that generating hydroguinones with lower O-H BDFEs could be a route to increased activity in future studies.

3.2. Directing Selectivity for ETPMs with Weak X-H Bonds

There is an important limiting factor to targeting a specific reaction driving force for HAT or concerted proton-electron transfers, depending on desired product selectivity. The formation of weak X–H bonds in an EPTM, while desirable for activating relatively inert substrates, can lead to the competitive evolution of H₂ through homolytic pathways. This parasitic pathway is evident in the work of Chalkley *et al.*, who identified that C–H bonds with a calculated BDFE of 31 kcal/mol form when CoCp*₂ is combined with ammonium-based acids.⁵⁰ Generating an activated EPTM which contains an X–H bond with low BDFE is essential to achieving N₂RR to NH₃ mediated by Fe tris(phosphino)borane complexes: the gas phase reduction of N₂ with three equivalents of H₂, requires an average BDFE of 49.9 kcal/mol.⁹⁴ Although the BDFE value for H₂ is not known in the diethyl ether solvent used by Chalkley *et al.* during co-electrocatalysis, its value in the related ethereal solvent THF is 52.0 kcal/mol.¹¹¹ Therefore, in all cases during electrocatalytic N₂RR the thermodynamically preferred formation of H₂ occurred, in some instances with competitive Faradaic efficiency to the desired NH₃ product.⁵⁰ Given the existing knowledge of the reaction landscape for the multistep transformation of N₂ to NH₃, potential opportunities exist for kinetic interception strategies that could outcompete competitive H₂ formation in the future.^{50,51,70,72}

Galvin and Waymouth⁴⁸ and McLoughlin et al.⁴⁹ have demonstrated the validity of this approach in the development of two transition metal-catalyzed catalyst systems for the AOR. For the example reported by McLoughlin et al., knowledge of the intrinsic mechanism of the mononuclear catalytic cycle mediated by the Ru complex was valuable, as metal hydride BDFEs generally fall in a relatively narrow range, which enabled more targeted selection of an EPTM. 120, 121 Thus, an additional Ru-based complex capable of HAT at a ligand-based radical reported by Wu et al. 122 could be identified with suitable properties for enabling co-electrocatalysis. In order to avoid the energetic penalty of oxidizing the Ru-based catalyst twice, the EPTM needed to be oxidized at more negative potentials than the Ru(II) hydride intermediate, possess a p K_a that was too weak to protonate the intermediate Ru(II) hydride to generate dihydrogen, and have a BDFE similar enough to the hydride to thermodynamically favor HAT from the Ru(II) hydride. Selecting a suitable EPTM was possible because some these values vary relatively little across solvents (e.g., metal hydride BDFE^{120, 121}) and other thermodynamic parameters can scale reasonably well across solvents (e.g., pK_a^{123}). It is worth noting that this approach can also result in mechanistic changes¹²⁴ and the best approach for success is undoubtedly one where experimentally measured values under relevant conditions have been established a priori. The design rules described by McLoughlin et al. are nonetheless quite effective for narrowing the EPTM screening process. Importantly, this strategy is generalizable to reductive processes as well: Derosa et al.

utilized a similar strategy based on the knowledge of M–H BDFEs to identify a RM that would generate M–H species *en route* to the reduction of CO₂ to formic acid.⁵²

3.3. Redox Potential Requirements for Co-Electrocatalysis

In contrast to these studies is the work of Smith et al., 56 where the fundamental reaction step differs from a conventional HAT or a concerted proton and electron transfer step. The role of pyridine derivatives to act as catalysts for CO₂ reduction inspires debate. 46 however, Smith et al. focused on the generation of dihydropyridines which did not have sufficient hydricity to react with CO₂ on their own. 125, 126 Therefore, as a design principle, the mediator was to transfer protons and electrons to the intermediates generated when CO₂ binds to [Fe(TPP)]²⁻ in the presence of proton donors. In the proposed mechanism for the CO₂RR mediated by [Fe(TPP)]⁺, catalysis is initiated upon the generation of an 'Fe(0)' species at the electrode, [Fe(TPP)]²⁻ (Figure 15). 127 Upon CO₂ binding, the resultant [Fe(TPP)(•CO₂)]²⁻ adduct is stabilized by an equilibrium hydrogen bonding interaction with the proton donor in solution $K_{AH 1}$, nota bene at low concentrations of added acid the catalytic current becomes second-order with respect to [acid]. This stabilization impacts K_{CO2} , particularly in ligand frameworks with positioned charged moieties or proton and hydrogen bond donors, which can have profound effects on the observed electrocatalytic response. 91, 106, 128 Subsequently, a second proton donor association triggers electron transfer from the Fe center, with concomitant bond cleavage to generate the H₂O co-product and a formally Fe(II) carbonyl species. The release of CO then occurs via a comproportionation reaction with [Fe(TPP)]²⁻, completing the cycle.

[Fe(TPP)]⁻ + CO

[Fe(TPP)]⁻
$$K_{CO}$$

[Fe(TPP)]²

[Fe(TPP)]²
 K_{CO2}
 K_{CO2}

Figure 15. Previously proposed mechanism for CO₂RR by [Fe(TPP)]⁺. ¹²⁹

Since an increase in catalytic current is observed when the reducible pyridine derivatives are added to the reaction, we can speculate that it is the rate-determining C-OH bond cleavage event that is being impacted. One possibility is that the favorable association of the EPTM to $[Fe(TPP)(\bullet CO_2)]^{2-}$ through hydrogen-bonding interactions supplants K_{AH_1} and the non-covalent interaction of the activated EPTM (a theoretical two-proton and two-electron donor) with metalbound substrate can shunt the catalytic cycle directly back to [Fe(TPP)]²⁻ with CO and H₂O loss. Since these conditions include PhOH, which serves as a competent proton donor for the catalytic cycle depicted in Figure 15, there are likely to be contributions from the overlapping catalytic and co-catalytic mechanisms in the observed current. Modulation of EPTM equilibrium association to $[Fe(TPP)(\cdot CO_2)]^{2-}$ relative to $K_{AH 1}$ would then be expected to shift the observed catalytic rate through control of the relative concentrations of the two possible active species in solution. This proposal is supported by the observation that the reduction potential of the EPTM needs to be slightly positive of that for the catalyst for the greatest enhancement to occur. Generating the reduced RM at potentials positive of the catalytic wave is advantageous for generating sufficient concentrations of the activated EPTM to compensate for the presumably sluggish kinetics of the 2H⁺/2e⁻ transfer during the co-catalytic cycle. This proposal suggests that the inclusion of stronger hydrogen bond donors on the EPTM should cause greater rate enhancements.

Our mechanistic analysis of the Cr(N₂O₂)/DBTD system initially suggested that the distinction between inner- or outer-sphere electron transfer by the RM in the catalytic cycle could not be clearly defined, since the RM reduction potentials were more negative than the intrinsic catalytic response.^{57, 58} However, the balance between the intrinsic and co-catalytic cycles was found to be connected to the favorability of the equilibrium association of the RM to the catalyst (Figure **16**).⁵⁹ Interestingly, RMs with more positive reduction potentials resulted in greater coelectrocatalytic activity, a form of inverse potential scaling. This observation suggests that a component of forming strong PB is the energetic matching of the participating aromatic components, in addition to the components possessing steric profiles which favor strong orbital overlap and significant dispersion effects. The Cr(N₂O₂)/DBTD co-electrocatalytic system differs from the others in that electron transfer unaccompanied by a proton is proposed to occur between the RM and metal center. However, it allows a dianionic species to be generated at potentials approximately 0.5 V more positive than is possible in the intrinsic Cr-based catalytic cycle, which, like the other approaches discussed above, results in the generation of a more reactive catalyst species at less negative potentials because of the cooperative interaction of two redox-active components. This suggests that further activity increases will be possible by achieving

overlapping reduction potentials for the catalyst and RM, as well as by introducing greater aromatic character to each.

Figure 16. Proposed catalytic mechanism for co-electrocatalytic CO₂ reduction by Cr and RM under protic conditions. Adapted from Ref. ⁵⁹ with permission from the Royal Society of Chemistry.

4. Conclusions and Outlook

Overall, the relatively limited examples described above suggest that the identification of simple thermodynamic values from catalytic cycles is of continuing importance to guide exploratory screening of possible mediators. The logical manifestation of this idea is found in the work of McLoughlin *et al.*, who have selected a series of parameters for the identification of possible RMs for the AOR. Particularly compelling is their use of a transition metal complex as an EPTM, which they emphasize is attractive relative to organic molecules "...because the thermochemical properties (BDFE, pK_a , $E_{1/2}$) of these complexes can be readily modified by changing the nature of the ligand(s) and/or redox-active transition metal." The importance of understanding the reaction landscape and the most prominent features is essential for this approach, as it is no coincidence that many of the co-electrocatalytic strategies discussed above access lower energy pathways by avoiding metal-based two-electron events to favor two distributed one-electron events. For kinetic and thermodynamic reasons, the movement of

electrons with protons can also offer significant advantages, as can shifting the redox reactions from outer- to inner-sphere (**Figure 17**).

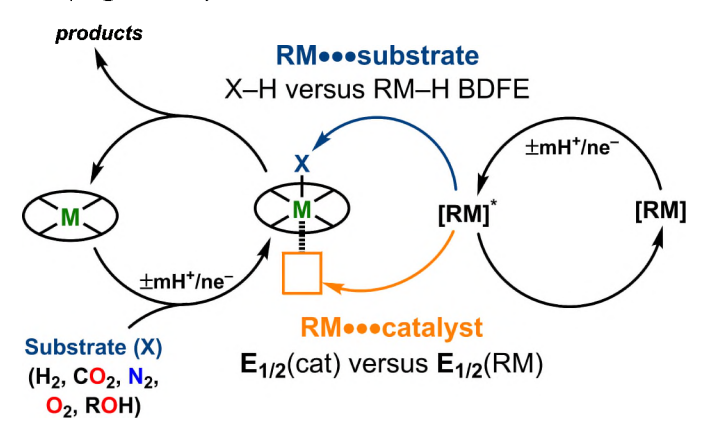


Figure 17. Overview of the ways in which RMs can interact with the catalytic species and parameters dictating this role.

The adaptation of aerobic reactions that use small molecule mediators to use electrodes to supply the necessary electrons or oxidizing equivalents has proven to be a powerful strategy for identifying new co-electrocatalytic electrochemical reactions.^{5, 6, 38} However, there exists a multitude of molecular transformations that rely on the stoichiometric inclusion of reductants and oxidants that would benefit from electrification. Indeed, ferrocene derivatives have begun attracting attention as mediators in electrocatalytic oxidative transformations where the regeneration and stabilization of the catalytically active species is required^{62, 130} or where catalystbound substrates can be activated. 131 As mentioned in the introduction, the ability of ferrocenes to function as catalytic electron-transfer mediators is also well established, 30-32 but these are not co-catalytic systems, and the mechanisms do not require inner-sphere electron transfer events. 132 We emphasize again that the limitation of the 50 mV separation identified in biological systems does not necessarily exist in abiotic ones.⁵⁷⁻⁵⁹ In biological systems with a variety of overlapping reaction pathways, selectivity is enforced by establishing energy gradients with gradual steps. However, synthetic reaction conditions can be specifically tailored such that reactions with larger driving forces can selectively occur, assuming this has a benefit on kinetic parameters¹¹⁷ and does not introduce large energy penalties. However, there are still additional challenges that must be addressed when designing co-electrocatalytic systems. As is the case with many complex chemical systems, there is the possibility of a competitive reaction pathway when introducing a RM such as direct reaction of the RM with substrate or interaction of the RM with catalytic intermediates outside of the step of interest which can lead to side products or deactivation of the active catalyst.

Lastly, we can consider what the field needs to accomplish moving forward in this area. An objection to these systems could be articulated thusly: why develop multicomponent co-catalytic systems instead of single component ones with ligand frameworks that directly incorporate RM elements? In redox-active catalyst systems, the coupling of redox-active moieties to active sites can indeed impact activity in a beneficial way, 133-136 however the intrinsic redox response of any molecule reflects electronic interactions between the two components prior to reduction. Ignoring the potential synthetic challenges, spatially co-locating multiple redox-active moieties can be an intrinsic limitation to improving catalysis, given that the function of both the redox-active fragment and catalyst will change! Therefore, we believe there is continued value in understanding intrinsic catalytic cycles and using principles of molecular design to select secondary components, which impact catalyst speciation and the shunting of mechanistic pathways as described above. Given the density of information available about aerobic catalytic processes and those which use stoichiometric reductants or oxidants, we advocate for further studies on RM-based electrification of synthetic transformations. Likewise, with many well-established electrocatalysts for small molecule activation, it is surprising that so few co-catalytic examples exist, given the obvious precedents discussed in the introduction. Here, too, mechanistic information can allow for analogous advances, as we begin to better understand how electrons and protons shift during a reaction such that we can better direct their selective transfer.

Funding Sources

The research of the authors' discussed in this perspective has been supported by the following funders: University of Virginia; U.S. Department of Energy, Office of Science, Office of Basic Energy Sciences, Catalysis Science Program, under Award DE-SC0022219, N.S.F. CHE-2102156 and ACS PRF 61430-ND3.

References

- 1. Kopylovich, M. N.; Ribeiro, A. P. C.; Alegria, E. C. B. A.; Martins, N. M. R.; Martins, L. M. D. R. S.; Pombeiro, A. J. L., Chapter Three Catalytic Oxidation of Alcohols: Recent Advances. In *Adv. Organomet. Chem.*, Pérez, P. J., Ed. Academic Press: 2015; Vol. 63, pp 91-174.
- 2. Guo, X.; Du, H.; Qu, F.; Li, J., Recent progress in electrocatalytic nitrogen reduction. *J. Mater. Chem. A* **2019**, *7* (8), 3531-3543.
- 3. Pegis, M. L.; Wise, C. F.; Martin, D. J.; Mayer, J. M., Oxygen Reduction by Homogeneous Molecular Catalysts and Electrocatalysts. *Chem. Rev.* **2018**, *118* (5), 2340-2391.
- 4. Francke, R.; Schille, B.; Roemelt, M., Homogeneously Catalyzed Electroreduction of Carbon Dioxide—Methods, Mechanisms, and Catalysts. *Chem. Rev.* **2018**, *118* (9), 4631-4701.
- 5. Badalyan, A.; Stahl, S. S., Cooperative electrocatalytic alcohol oxidation with electron-proton-transfer mediators. *Nature* **2016**, *535* (7612), 406-410.
- 6. Anson, C. W.; Stahl, S. S., Cooperative Electrocatalytic O₂ Reduction Involving Co(salophen) with p-Hydroquinone as an Electron–Proton Transfer Mediator. *J. Am. Chem. Soc.* **2017**, *139* (51), 18472-18475.
- 7. Kristensen, S. B.; van Mourik, T.; Pedersen, T. B.; Sørensen, J. L.; Muff, J., Simulation of electrochemical properties of naturally occurring quinones. *Sci. Rep.* **2020**, *10* (1), 13571.
- 8. Alcázar-Fabra, M.; Navas, P.; Brea-Calvo, G., Coenzyme Q biosynthesis and its role in the respiratory chain structure. *Biochim. Biophys. Acta Bioenerg* **2016**, *1857* (8), 1073-1078.
- 9. Chen, H.; Simoska, O.; Lim, K.; Grattieri, M.; Yuan, M.; Dong, F.; Lee, Y. S.; Beaver, K.; Weliwatte, S.; Gaffney, E. M.; Minteer, S. D., Fundamentals, Applications, and Future Directions of Bioelectrocatalysis. *Chem. Rev.* **2020**, *120* (23), 12903-12993.
- 10. Schneider, C. R.; Shafaat, H. S., An internal electron reservoir enhances catalytic CO₂ reduction by a semisynthetic enzyme. *ChemComm* **2016**, *52* (64), 9889-9892.
- 11. Johnson, D. C.; Dean, D. R.; Smith, A. D.; Johnson, M. K., STRUCTURE, FUNCTION, AND FORMATION OF BIOLOGICAL IRON-SULFUR CLUSTERS. *Annu. Rev. Biochem.* **2005**, 74, 247-81.
- 12. Ibrahim, I. M.; Wu, H.; Ezhov, R.; Kayanja, G. E.; Zakharov, S. D.; Du, Y.; Tao, W. A.; Pushkar, Y.; Cramer, W. A.; Puthiyaveetil, S., An evolutionarily conserved iron-sulfur cluster underlies redox sensory function of the Chloroplast Sensor Kinase. *Commun. Biol.* **2020**, *3* (1), 13.
- 13. Silveira, C. M.; Almeida, M. G., Small electron-transfer proteins as mediators in enzymatic electrochemical biosensors. *Anal. Bioanal. Chem.* **2013**, *405* (11), 3619-3635.
- 14. Nöll, T.; Nöll, G., Strategies for "wiring" redox-active proteins to electrodes and applications in biosensors, biofuel cells, and nanotechnology. *Chem. Soc. Rev.* **2011**, *40* (7), 3564-3576.
- 15. Heller, A.; Feldman, B., Electrochemical Glucose Sensors and Their Applications in Diabetes Management. *Chem. Rev.* **2008**, *108* (7), 2482-2505.
- 16. Abasıyanık, M. F.; Şenel, M., Immobilization of glucose oxidase on reagentless ferrocene-containing polythiophene derivative and its glucose sensing application. *J. Electroanal. Chem.* **2010**, 639 (1), 21-26.
- 17. De Wael, K.; Bashir, Q.; Van Vlierberghe, S.; Dubruel, P.; Heering, H. A.; Adriaens, A., Electrochemical determination of hydrogen peroxide with cytochrome *c* peroxidase and horse heart cytochrome *c* entrapped in a gelatin hydrogel. *Bioelectrochemistry* **2012**, *83*, 15-18.
- 18. Dronov, R.; Kurth, D. G.; Scheller, F. W.; Lisdat, F., Direct and Cytochrome c Mediated Electrochemistry of Bilirubin Oxidase on Gold. *Electroanalysis* **2007**, *19* (15), 1642-1646.
- 19. Gong, J.; Liu, W.; Du, X.; Liu, C.; Zhang, Z.; Sun, F.; Yang, L.; Xu, D.; Guo, H.; Deng, Y., Direct Conversion of Wheat Straw into Electricity with a Biomass Flow Fuel Cell Mediated by Two Redox Ion Pairs. *ChemSusChem* **2017**, *10* (3), 506-513.

- 20. Zu, X.; Sun, L.; Gong, J.; Liu, X.; Liu, Y.; Du, X.; Liu, W.; Chen, L.; Yi, G.; Zhang, W.; Lin, W.; Li, W.; Deng, Y., Ferric ion pair mediated biomass redox flow fuel cell and related chemical reaction kinetics study. *Chem. Eng. J.* **2018**, *348*, 476-484.
- 21. Lamb, A. B.; Elder, L. W., THE ELECTROMOTIVE ACTIVATION OF OXYGEN. *J. Am. Chem. Soc.* **1931**, *53* (1), 137-163.
- 22. Kummer, J. T.; Oei, D. G., A chemically regenerative redox fuel cell. II. *J. Appl. Electrochem.* **1985**, *15* (4), 619-629.
- 23. Zhao, X.; Zhu, J. Y., Efficient Conversion of Lignin to Electricity Using a Novel Direct Biomass Fuel Cell Mediated by Polyoxometalates at Low Temperatures. *ChemSusChem* **2016**, 9 (2), 197-207.
- 24. Bergens, S. H.; Gorman, C. B.; Palmore, G. T. R.; Whitesides, G. M., A Redox Fuel-Cell That Operates with Methane as Fuel at 120-Degrees-C. *Science* **1994**, *265* (5177), 1418-1420.
- 25. Gorman, C. B.; Bergens, S. H.; Whitesides, G. M., Platinum-Catalyzed Oxidations of Organic Compounds by Ferric Sulfate: Use of a Redox Fuel Cell to Mediate Complete Oxidation of Ethylene Glycol by Dioxygen at 80°C. *J. Catal.* **1996**, *158* (1), 92-96.
- 26. Anson, C. W.; Stahl, S. S., Mediated Fuel Cells: Soluble Redox Mediators and Their Applications to Electrochemical Reduction of O₂ and Oxidation of H₂, Alcohols, Biomass, and Complex Fuels. *Chem. Rev.* **2020**, *120* (8), 3749-3786.
- 27. Milton, R. D.; Cai, R.; Abdellaoui, S.; Leech, D.; De Lacey, A. L.; Pita, M.; Minteer, S. D., Bioelectrochemical Haber–Bosch Process: An Ammonia-Producing H2/N2 Fuel Cell. *Angew. Chem., Int. Ed.* **2017**, *56* (10), 2680-2683.
- 28. Silverstein, T. P., Marcus Theory: Thermodynamics CAN Control the Kinetics of Electron Transfer Reactions. *J. Chem. Educ.* **2012**, *89* (9), 1159-1167.
- 29. Piechota, E. J.; Meyer, G. J., Introduction to Electron Transfer: Theoretical Foundations and Pedagogical Examples. *J. Chem. Educ.* **2019**, *96* (11), 2450-2466.
- 30. Lennox, A. J. J.; Nutting, J. E.; Stahl, S. S., Selective electrochemical generation of benzylic radicals enabled by ferrocene-based electron-transfer mediators. *Chem. Sci.* **2018**, 9 (2), 356-361.
- 31. Zhu, L.; Xiong, P.; Mao, Z.-Y.; Wang, Y.-H.; Yan, X.; Lu, X.; Xu, H.-C., Electrocatalytic Generation of Amidyl Radicals for Olefin Hydroamidation: Use of Solvent Effects to Enable Anilide Oxidation. *Angew. Chem.*, *Int. Ed.* **2016**, *55* (6), 2226-2229.
- 32. Wu, Z.-J.; Xu, H.-C., Synthesis of C3-Fluorinated Oxindoles through Reagent-Free Cross-Dehydrogenative Coupling. *Angew. Chem., Int. Ed.* **2017**, *56* (17), 4734-4738.
- 33. Francke, R.; Little, R. D., Redox catalysis in organic electrosynthesis: basic principles and recent developments. *Chem. Soc. Rev.* **2014**, *43* (8), 2492-2521.
- 34. Wang, F.; Gerken, J. B.; Bates, D. M.; Kim, Y. J.; Stahl, S. S., Electrochemical Strategy for Hydrazine Synthesis: Development and Overpotential Analysis of Methods for Oxidative N–N Coupling of an Ammonia Surrogate. *J. Am. Chem. Soc.* **2020**, *142* (28), 12349-12356.
- 35. Nutting, J. E.; Rafiee, M.; Stahl, S. S., Tetramethylpiperidine N-Oxyl (TEMPO), Phthalimide N-Oxyl (PINO), and Related N-Oxyl Species: Electrochemical Properties and Their Use in Electrocatalytic Reactions. *Chem. Rev.* **2018**, *118* (9), 4834-4885.
- 36. McCann, S. D.; Stahl, S. S., Copper-Catalyzed Aerobic Oxidations of Organic Molecules: Pathways for Two-Electron Oxidation with a Four-Electron Oxidant and a One-Electron Redox-Active Catalyst. *Acc. Chem. Res.* **2015**, *48* (6), 1756-1766.
- 37. Hoover, J. M.; Ryland, B. L.; Stahl, S. S., Mechanism of Copper(I)/TEMPO-Catalyzed Aerobic Alcohol Oxidation. *J. Am. Chem. Soc.* **2013**, *135* (6), 2357-2367.
- 38. Wang, F.; Stahl, S. S., Electrochemical Oxidation of Organic Molecules at Lower Overpotential: Accessing Broader Functional Group Compatibility with Electron-Proton Transfer Mediators. *Acc. Chem. Res.* **2020**, *53* (3), 561-574.

- 39. Shan, B.; Schmehl, R., Photochemical Generation of Strong One-Electron Reductants via Light-Induced Electron Transfer with Reversible Donors Followed by Cross Reaction with Sacrificial Donors. *J. Phys. Chem. A* **2014**, *118* (45), 10400-10406.
- 40. Tyson, E. L.; Niemeyer, Z. L.; Yoon, T. P., Redox Mediators in Visible Light Photocatalysis: Photocatalytic Radical Thiol–Ene Additions. *J. Org. Chem.* **2014**, 79 (3), 1427-1436.
- 41. Happ, B.; Winter, A.; Hager, M. D.; Schubert, U. S., Photogenerated avenues in macromolecules containing Re(I), Ru(II), Os(II), and Ir(III) metal complexes of pyridine-based ligands. *Chem. Soc. Rev.* **2012**, *41* (6), 2222-2255.
- 42. Andreiadis, E. S.; Chavarot-Kerlidou, M.; Fontecave, M.; Artero, V., Artificial Photosynthesis: From Molecular Catalysts for Light-driven Water Splitting to Photoelectrochemical Cells. *Photochem. Photobiol.* **2011**, *87* (5), 946-964.
- 43. Teets, T. S.; Nocera, D. G., Photocatalytic hydrogen production. *Chem. Commun.* **2011**, 47 (33), 9268-9274.
- 44. Sakai, K.; Ozawa, H., Homogeneous catalysis of platinum(II) complexes in photochemical hydrogen production from water. *Coord. Chem. Rev.* **2007**, *251* (21), 2753-2766.
- 45. Oh, Y.; Hu, X. L., Organic molecules as mediators and catalysts for photocatalytic and electrocatalytic CO₂ reduction. *Chem. Soc. Rev.* **2013**, *42* (6), 2253-2261.
- 46. Vasilyev, D. V.; Dyson, P. J., The Role of Organic Promoters in the Electroreduction of Carbon Dioxide. *ACS Catal.* **2021**, *11* (3), 1392-1405.
- 47. Koval, C. A.; Lercher, J.; Scott, S. L.; Coates, G. W.; Iglesia, E.; Bullock, R. M.; Jaramillo, T. F.; Flytzani-Stephanopoulos, M.; Resasco, D.; Tway, C. L.; Batista, V.; Chapman, K. W.; Dai, S.; Dumesic, J.; Friend, C.; Hille, R.; Johnson, K.; Nørskov, J.; Rekoske, J.; Sarkar, R.; Bradley, C.; Garrett, B.; Henderson, C.; Miranda, R.; Peden, C.; Schwartz, V.; Runkles, K.; Fellner, K.; Jenks, C.; Nelson, M.; Appel, A. M.; Bare, S.; Bartlett, B. M.; Bligaard, T.; Chandler, B. D.; Davis, R. J.; Glezakou, V.-A.; Gregoire, J.; Hille, R.; Hock, A. S.; Kitchin, J.; Kung, H. H.; Rousseau, R.; Sadow, A. D.; Schaak, R. E.; Shaw, W. J.; Stacchiola, D. J.; Delferro, M.; Bunel, E.; Holladay, J.; Houle, F.; Jenks, C.; Krause, T.; Marshall, C.; Neale, N.; Parks, J.; Schaidle, J.; VandeLagemaat, J.; Wang, Y.; Weber, R. Basic Research Needs for Catalysis Science to Transform Energy Technologies: Report from the U.S. Department of Energy, Office of Basic Energy Sciences Workshop May 8–10, 2017, in Gaithersburg, Maryland; United States, 2017-05-08, 2017.
- 48. Galvin, C. M.; Waymouth, R. M., Electron-Rich Phenoxyl Mediators Improve Thermodynamic Performance of Electrocatalytic Alcohol Oxidation with an Iridium Pincer Complex. *J. Am. Chem. Soc.* **2020**, *142* (45), 19368-19378.
- 49. McLoughlin, E. A.; Armstrong, K. C.; Waymouth, R. M., Electrochemically Regenerable Hydrogen Atom Acceptors: Mediators in Electrocatalytic Alcohol Oxidation Reactions. *ACS Catal.* **2020**, *10* (19), 11654-11662.
- 50. Chalkley, M. J.; Del Castillo, T. J.; Matson, B. D.; Peters, J. C., Fe-Mediated Nitrogen Fixation with a Metallocene Mediator: Exploring pKa Effects and Demonstrating Electrocatalysis. *J. Am. Chem. Soc.* **2018**, *140* (19), 6122-6129.
- 51. Garrido-Barros, P.; Derosa, J.; Chalkley, M. J.; Peters, J. C., Tandem electrocatalytic N₂ fixation via proton-coupled electron transfer. *Nature* **2022**, *609* (7925), 71-76.
- 52. Derosa, J.; Garrido-Barros, P.; Li, M.; Peters, J. C., Use of a PCET Mediator Enables a Ni-HER Electrocatalyst to Act as a Hydride Delivery Agent. *J. Am. Chem. Soc.* **2022**, *144* (43), 20118-20125.
- 53. Chambers, G. M.; Wiedner, E. S.; Bullock, R. M., H₂ Oxidation Electrocatalysis Enabled by Metal-to-Metal Hydrogen Atom Transfer: A Homolytic Approach to a Heterolytic Reaction. *Angew. Chem., Int. Ed.* **2018**, *57* (41), 13523-13527.

- 54. Hooe, S. L.; Cook, E. N.; Reid, A. G.; Machan, C. W., Non-covalent assembly of proton donors and p-benzoquinone anions for co-electrocatalytic reduction of dioxygen. *Chem. Sci.* **2021**, *12*, 9733-9741.
- 55. Gerken, J. B.; Stahl, S. S., High-Potential Electrocatalytic O₂ Reduction with Nitroxyl/NO_x Mediators: Implications for Fuel Cells and Aerobic Oxidation Catalysis. *ACS Cent. Sci.* **2015**, *1* (5), 234-243.
- 56. Smith, P. T.; Weng, S.; Chang, C. J., An NADH-Inspired Redox Mediator Strategy to Promote Second-Sphere Electron and Proton Transfer for Cooperative Electrochemical CO₂ Reduction Catalyzed by Iron Porphyrin. *Inorg. Chem.* **2020**, 59 (13), 9270-9278.
- 57. Hooe, S. L.; Moreno, J. J.; Reid, A. G.; Cook, E. N.; Machan, C. W., Mediated Inner-Sphere Electron Transfer Induces Homogeneous Reduction of CO₂ via Through-Space Electronic Conjugation**. *Angew. Chem., Int. Ed.* **2022**, *61* (1), e202109645.
- 58. Hooe, S. L.; Moreno, J. J.; Reid, A. G.; Cook, E. N.; Machan, C. W., Corrigendum: Mediated Inner-Sphere Electron Transfer Induces Homogeneous Reduction of CO₂ via Through-Space Electronic Conjugation. *Angew. Chem., Int. Ed.* **2022**, *61* (25), e202205139.
- 59. Reid, A. G.; Moreno, J. J.; Hooe, S. H.; Baugh, K. R.; Thomas, I. H.; Dickie, D. A.; Machan, C. W., Inverse Potential Scaling in Co-Electrocatalytic Activity for CO₂ Reduction Through Redox Mediator Tuning and Catalyst Design. *Chem. Sci.* **2022**, *13*, 9595-9606.
- 60. Dey, S.; Masero, F.; Brack, E.; Fontecave, M.; Mougel, V., Electrocatalytic metal hydride generation using CPET mediators. *Nature* **2022**, *607* (7919), 499-506.
- 61. Walker, B. R.; Manabe, S.; Brusoe, A. T.; Sevov, C. S., Mediator-Enabled Electrocatalysis with Ligandless Copper for Anaerobic Chan–Lam Coupling Reactions. *J. Am. Chem. Soc.* **2021**, *143* (16), 6257-6265.
- 62. Lee, K. J.; Lodaya, K. M.; Gruninger, C. T.; Rountree, E. S.; Dempsey, J. L., Redox mediators accelerate electrochemically-driven solubility cycling of molecular transition metal complexes. *Chem. Sci.* **2020**, *11* (36), 9836-9851.
- 63. Ciriminna, R.; Palmisano, G.; Pagliaro, M., Electrodes Functionalized with the 2,2,6,6-Tetramethylpiperidinyloxy Radical for the Waste-Free Oxidation of Alcohols. *ChemCatChem* **2015**, 7 (4), 552-558.
- 64. Bobbitt, J. M.; BrüCkner, C.; Merbouh, N., Oxoammonium- and Nitroxide-Catalyzed Oxidations of Alcohols. *Org. React.* **2010**, 103-424.
- 65. Semmelhack, M. F.; Chou, C. S.; Cortes, D. A., Nitroxyl-mediated electrooxidation of alcohols to aldehydes and ketones. *J. Am. Chem. Soc.* **1983**, *105* (13), 4492-4494.
- 66. Rafiee, M.; Miles, K. C.; Stahl, S. S., Electrocatalytic Alcohol Oxidation with TEMPO and Bicyclic Nitroxyl Derivatives: Driving Force Trumps Steric Effects. *J. Am. Chem. Soc.* **2015**, *137* (46), 14751-14757.
- 67. Hickey, D. P.; Schiedler, D. A.; Matanovic, I.; Doan, P. V.; Atanassov, P.; Minteer, S. D.; Sigman, M. S., Predicting Electrocatalytic Properties: Modeling Structure—Activity Relationships of Nitroxyl Radicals. *J. Am. Chem. Soc.* **2015**, *137* (51), 16179-16186.
- 68. Speelman, A. L.; Gerken, J. B.; Heins, S. P.; Wiedner, E. S.; Stahl, S. S.; Appel, A. M., Determining overpotentials for the oxidation of alcohols by molecular electrocatalysts in non-aqueous solvents. *Energy Environ. Sci.* **2022**, *15* (10), 4015-4024.
- 69. Waldie, K. M.; Flajslik, K. R.; McLoughlin, E.; Chidsey, C. E. D.; Waymouth, R. M., Electrocatalytic Alcohol Oxidation with Ruthenium Transfer Hydrogenation Catalysts. *J. Am. Chem. Soc.* **2017**, *139* (2), 738-748.
- 70. Matson, B. D.; Peters, J. C., Fe-Mediated HER vs N_2RR : Exploring Factors That Contribute to Selectivity in $P_3^EFe(N_2)$ (E = B, Si, C) Catalyst Model Systems. *ACS Catal.* **2018**, 8 (2), 1448-1455.
- 71. Chalkley, M. J.; Drover, M. W.; Peters, J. C., Catalytic N₂-to-NH₃ (or -N₂H₄) Conversion by Well-Defined Molecular Coordination Complexes. *Chem. Rev.* **2020**, *120* (12), 5582-5636.

- 72. Chalkley, M. J.; Del Castillo, T. J.; Matson, B. D.; Roddy, J. P.; Peters, J. C., Catalytic N₂-to-NH₃ Conversion by Fe at Lower Driving Force: A Proposed Role for Metallocene-Mediated PCET. *ACS Cent. Sci.* **2017**, *3* (3), 217-223.
- 73. Anson, C. W.; Ghosh, S.; Hammes-Schiffer, S.; Stahl, S. S., Co(salophen)-Catalyzed Aerobic Oxidation of p-Hydroquinone: Mechanism and Implications for Aerobic Oxidation Catalysis. *J. Am. Chem. Soc.* **2016**, *138* (12), 4186-4193.
- 74. Nitopi, S.; Bertheussen, E.; Scott, S. B.; Liu, X.; Engstfeld, A. K.; Horch, S.; Seger, B.; Stephens, I. E. L.; Chan, K.; Hahn, C.; Nørskov, J. K.; Jaramillo, T. F.; Chorkendorff, I., Progress and Perspectives of Electrochemical CO₂ Reduction on Copper in Aqueous Electrolyte. *Chem. Rev.* **2019**, *119* (12), 7610-7672.
- 75. Hooe, S. L.; Rheingold, A. L.; Machan, C. W., Electrocatalytic Reduction of Dioxygen to Hydrogen Peroxide by a Molecular Manganese Complex with a Bipyridine-Containing Schiff Base Ligand. *J. Am. Chem. Soc.* **2018**, *140* (9), 3232-3241.
- 76. Hooe, S. L.; Machan, C. W., Dioxygen Reduction to Hydrogen Peroxide by a Molecular Mn Complex: Mechanistic Divergence between Homogeneous and Heterogeneous Reductants. *J. Am. Chem. Soc.* **2019**, *141* (10), 4379-4387.
- 77. Huynh, M. T.; Anson, C. W.; Cavell, A. C.; Stahl, S. S.; Hammes-Schiffer, S., Quinone 1 e⁻ and 2 e⁻/2 H⁺ Reduction Potentials: Identification and Analysis of Deviations from Systematic Scaling Relationships. *J. Am. Chem. Soc.* **2016**, *138* (49), 15903-15910.
- 78. Gupta, N.; Linschitz, H., Hydrogen-Bonding and Protonation Effects in Electrochemistry of Quinones in Aprotic Solvents. *J. Am. Chem. Soc.* **1997**, *119* (27), 6384-6391.
- 79. Costentin, C., Electrochemical Approach to the Mechanistic Study of Proton-Coupled Electron Transfer. *Chem. Rev.* **2008**, *108* (7), 2145-2179.
- 80. Quan, M.; Sanchez, D.; Wasylkiw, M. F.; Smith, D. K., Voltammetry of Quinones in Unbuffered Aqueous Solution: Reassessing the Roles of Proton Transfer and Hydrogen Bonding in the Aqueous Electrochemistry of Quinones. *J. Am. Chem. Soc.* **2007**, *129* (42), 12847-12856.
- 81. Staley, P. A.; Lopez, E. M.; Clare, L. A.; Smith, D. K., Kinetic Stabilization of Quinone Dianions via Hydrogen Bonding by Water in Aprotic Solvents. *J. Phys. Chem. C* **2015**, *119* (35), 20319-20327.
- 82. Evans, D. H., One-Electron and Two-Electron Transfers in Electrochemistry and Homogeneous Solution Reactions. *Chem. Rev.* **2008**, *108* (7), 2113-2144.
- 83. Astudillo, P. D.; Tiburcio, J.; González, F. J., The role of acids and bases on the electrochemical oxidation of hydroquinone: Hydrogen bonding interactions in acetonitrile. *J. Electroanal. Chem.* **2007**, *604* (1), 57-64.
- 84. Astudillo, P. D.; Valencia, D. P.; González-Fuentes, M. A.; Díaz-Sánchez, B. R.; Frontana, C.; González, F. J., Electrochemical and chemical formation of a low-barrier proton transfer complex between the quinone dianion and hydroquinone. *Electrochim. Acta* **2012**, *81*, 197-204.
- 85. Alligrant, T. M.; Hackett, J. C.; Alvarez, J. C., Acid/base and hydrogen bonding effects on the proton-coupled electron transfer of quinones and hydroquinones in acetonitrile: Mechanistic investigation by voltammetry, ¹H NMR and computation. *Electrochim. Acta* **2010**, *55* (22), 6507-6516.
- 86. Lam, Y. C.; Nielsen, R. J.; Gray, H. B.; Goddard, W. A., A Mn Bipyrimidine Catalyst Predicted To Reduce CO₂ at Lower Overpotential. *ACS Catal.* **2015**, *5* (4), 2521-2528.
- 87. Macías-Ruvalcaba, N. A.; Okumura, N.; Evans, D. H., Change in Reaction Pathway in the Reduction of 3,5-Di-*tert*-butyl-1,2-benzoquinone with Increasing Concentrations of 2,2,2-Trifluoroethanol. *J. Phys. Chem. B* **2006**, *110* (43), 22043-22047.
- 88. Evans, D. H.; René, A., Reinvestigation of a former concerted proton-electron transfer (CPET), the reduction of a hydrogen-bonded complex between a proton donor and the anion radical of 3,5-di-*tert*-butyl-1,2-benzoquinone. *Phys. Chem. Chem. Phys.* **2012**, *14* (14), 4844-4848.

- 89. Shi, R. S.; Tessensohn, M. E.; Lauw, S. J. L.; Foo, N. A. B. Y.; Webster, R. D., Tuning the reduction potential of quinones by controlling the effects of hydrogen bonding, protonation and proton-coupled electron transfer reactions. *ChemComm* **2019**, *55* (16), 2277-2280.
- 90. Cook, E. N.; Machan, C. W., Homogeneous Catalysis of Dioxygen Reduction by Molecular Mn Complexes. *ChemComm* **2022**, *58*, 11746-11761.
- 91. Nichols, E. M.; Derrick, J. S.; Nistanaki, S. K.; Smith, P. T.; Chang, C. J., Positional effects of second-sphere amide pendants on electrochemical CO₂ reduction catalyzed by iron porphyrins. *Chem. Sci.* **2018**, 9 (11), 2952-2960.
- 92. Nichols, E. M.; Chang, C. J., Urea-Based Multipoint Hydrogen-Bond Donor Additive Promotes Electrochemical CO₂ Reduction Catalyzed by Nickel Cyclam. *Organometallics* **2019**, 38 (6), 1213-1218.
- 93. Saveant, J. M.; Costentin, C., Elements of Molecular and Biomolecular Electrochemistry: An Electrochemical Approach to Electron Transfer Chemistry, 2nd Edition. *Elements of Molecular and Biomolecular Electrochemistry: An Electrochemical Approach to Electron Transfer Chemistry, 2nd Edition* **2019**, 1-616.
- 94. Agarwal, R. G.; Coste, S. C.; Groff, B. D.; Heuer, A. M.; Noh, H.; Parada, G. A.; Wise, C. F.; Nichols, E. M.; Warren, J. J.; Mayer, J. M., Free Energies of Proton-Coupled Electron Transfer Reagents and Their Applications. *Chem. Rev.* **2022**, *122* (1), 1-49.
- 95. Sampson, M. D.; Kubiak, C. P., Manganese Electrocatalysts with Bulky Bipyridine Ligands: Utilizing Lewis Acids To Promote Carbon Dioxide Reduction at Low Overpotentials. *J. Am. Chem. Soc.* **2016**, *138* (4), 1386-1393.
- 96. Sampson, M. D.; Nguyen, A. D.; Grice, K. A.; Moore, C. E.; Rheingold, A. L.; Kubiak, C. P., Manganese Catalysts with Bulky Bipyridine Ligands for the Electrocatalytic Reduction of Carbon Dioxide: Eliminating Dimerization and Altering Catalysis. *J. Am. Chem. Soc.* **2014**, *136* (14), 5460-5471.
- 97. Hooe, S. L.; Dressel, J. M.; Dickie, D. A.; Machan, C. W., Highly Efficient Electrocatalytic Reduction of CO₂ to CO by a Molecular Chromium Complex. *ACS Catal.* **2020**, *10* (2), 1146-1151.
- 98. Moreno, J. J.; Hooe, S. L.; Machan, C. W., DFT Study on the Electrocatalytic Reduction of CO₂ to CO by a Molecular Chromium Complex. *Inorg. Chem.* **2021**, *60* (6), 3635-3650.
- 99. Li, J.; Shen, P. Z., Zujin; Tang, Ben Z., Through-Space Conjugation: A Thriving Alternative for Optoelectronic Materials. *CCS Chem.* **2019**, *1* (2), 181-196.
- 100. Garcia-Yoldi, I.; Miller, J. S.; Novoa, J. J., Structure and Stability of the [TCNE]₂²⁻ Dimers in Dichloromethane Solution: A Computational Study. *J. Phys. Chem. A.* **2007**, *111* (32), 8020-8027.
- 101. Garcia-Yoldi, I.; Miller, J. S.; Novoa, J. J., [Cyanil]₂²⁻ dimers possess long, two-electron ten-center (2e⁻/10c) multicenter bonding. *Phys. Chem. Chem. Phys.* **2008**, *10* (28), 4106-4109.
- 102. Mota, F.; Miller, J. S.; Novoa, J. J., Comparative Analysis of the Multicenter, Long Bond in [TCNE] and Phenalenyl Radical Dimers: A Unified Description of Multicenter, Long Bonds. *J. Am. Chem. Soc.* **2009**, *131* (22), 7699-7707.
- 103. Kertesz, M., Pancake Bonding: An Unusual Pi-Stacking Interaction. *Chem. Eur. J.* **2019**, 25 (2), 400-416.
- 104. Kozuch, S.; Shaik, S., How to Conceptualize Catalytic Cycles? The Energetic Span Model. *Acc. Chem. Res.* **2011**, *44* (2), 101-110.
- 105. Costentin, C.; Savéant, J.-M., Homogeneous Molecular Catalysis of Electrochemical Reactions: Manipulating Intrinsic and Operational Factors for Catalyst Improvement. *J. Am. Chem. Soc.* **2018**, *140* (48), 16669-16675.
- 106. Azcarate, I.; Costentin, C.; Robert, M.; Saveant, J. M., Through-Space Charge Interaction Substituent Effects in Molecular Catalysis Leading to the Design of the Most Efficient Catalyst of CO₂-to-CO Electrochemical Conversion. *J. Am. Chem. Soc.* **2016**, *138* (51), 16639-16644.

- 107. Gotico, P.; Roupnel, L.; Guillot, R.; Sircoglou, M.; Leibl, W.; Halime, Z.; Aukauloo, A., Atropisomeric Hydrogen Bonding Control for CO₂ Binding and Enhancement of Electrocatalytic Reduction at Iron Porphyrins. *Angew. Chem.*, *Int. Ed.* **2020**, *59* (50), 22451-22455.
- 108. Nie, W.; Tarnopol, D. E.; McCrory, C. C. L., Enhancing a Molecular Electrocatalyst's Activity for CO₂ Reduction by Simultaneously Modulating Three Substituent Effects. *J. Am. Chem. Soc.* **2021**, *143* (10), 3764-3778.
- 109. Bordwell, F. G.; Bausch, M. J., Acidity-oxidation-potential (AOP) values as estimates of relative bond dissociation energies and radical stabilities in dimethyl sulfoxide solution. *J. Am. Chem. Soc.* **1986**, *108* (8), 1979-1985.
- 110. Bordwell, F. G.; Cheng, J. P.; Harrelson, J. A., Homolytic bond dissociation energies in solution from equilibrium acidity and electrochemical data. *J. Am. Chem. Soc.* **1988**, *110* (4), 1229-1231.
- 111. Wise, C. F.; Agarwal, R. G.; Mayer, J. M., Determining Proton-Coupled Standard Potentials and X–H Bond Dissociation Free Energies in Nonaqueous Solvents Using Open-Circuit Potential Measurements. *J. Am. Chem. Soc.* **2020**, *142* (24), 10681-10691.
- 112. Warren, J. J.; Tronic, T. A.; Mayer, J. M., Thermochemistry of Proton-Coupled Electron Transfer Reagents and its Implications. *Chem Rev* **2010**, *110* (12), 6961-7001.
- 113. Cuerva, J. M.; Campaña, A. G.; Justicia, J.; Rosales, A.; Oller-López, J. L.; Robles, R.; Cárdenas, D. J.; Buñuel, E.; Oltra, J. E., Water: The Ideal Hydrogen-Atom Source in Free-Radical Chemistry Mediated by TillI and Other Single-Electron-Transfer Metals? *Angew. Chem., Int. Ed.* **2006**, *45* (33), 5522-5526.
- 114. Blanksby, S. J.; Ellison, G. B., Bond Dissociation Energies of Organic Molecules. *Acc. Chem. Res.* **2003**, *36* (4), 255-263.
- 115. Ryland, B. L.; McCann, S. D.; Brunold, T. C.; Stahl, S. S., Mechanism of Alcohol Oxidation Mediated by Copper(II) and Nitroxyl Radicals. *J. Am. Chem. Soc.* **2014**, *136* (34), 12166-12173.
- 116. Ruscic, B., Active Thermochemical Tables: Sequential Bond Dissociation Enthalpies of Methane, Ethane, and Methanol and the Related Thermochemistry. *J. Phys. Chem. A* **2015**, *119* (28), 7810-7837.
- 117. Saouma, C. T.; Mayer, J. M., Do spin state and spin density affect hydrogen atom transfer reactivity? *Chem. Sci.* **2014**, *5* (1), 21-31.
- 118. Shaik, S.; Hirao, H.; Kumar, D., Reactivity of High-Valent Iron–Oxo Species in Enzymes and Synthetic Reagents: A Tale of Many States. *Acc. Chem. Res.* **2007**, *40* (7), 532-542.
- 119. Zhu, X.-Q.; Wang, C.-H.; Liang, H., Scales of Oxidation Potentials, pKa, and BDE of Various Hydroguinones and Catechols in DMSO. *J. Org. Chem. Res* **2010**, *75* (21), 7240-7257.
- 120. Wiedner, E. S.; Chambers, M. B.; Pitman, C. L.; Bullock, R. M.; Miller, A. J. M.; Appel, A. M., Thermodynamic Hydricity of Transition Metal Hydrides. *Chem. Rev.* **2016**, *116* (15), 8655-8692.
- 121. Waldie, K. M.; Ostericher, A. L.; Reineke, M. H.; Sasayama, A. F.; Kubiak, C. P., Hydricity of Transition-Metal Hydrides: Thermodynamic Considerations for CO₂ Reduction. *ACS Catal.* **2018**, *8* (2), 1313-1324.
- 122. Wu, A.; Masland, J.; Swartz, R. D.; Kaminsky, W.; Mayer, J. M., Synthesis and Characterization of Ruthenium Bis(β-diketonato) Pyridine-Imidazole Complexes for Hydrogen Atom Transfer. *Inorg. Chem.* **2007**, *46* (26), 11190-11201.
- 123. Kütt, A.; Tshepelevitsh, S.; Saame, J.; Lõkov, M.; Kaljurand, I.; Selberg, S.; Leito, I., Strengths of Acids in Acetonitrile. *Eur. J. Org. Chem.* **2021**, 2021 (9), 1407-1419.
- 124. Burgess, S. A.; Appel, A. M.; Linehan, J. C.; Wiedner, E. S., Changing the Mechanism for CO₂ Hydrogenation Using Solvent-Dependent Thermodynamics. *Angew. Chem., Int. Ed.* **2017**, *56* (47), 15002-15005.

- 125. Lim, C.-H.; Ilic, S.; Alherz, A.; Worrell, B. T.; Bacon, S. S.; Hynes, J. T.; Glusac, K. D.; Musgrave, C. B., Benzimidazoles as Metal-Free and Recyclable Hydrides for CO₂ Reduction to Formate. *J. Am. Chem. Soc.* **2019**, *141* (1), 272-280.
- 126. Ilic, S.; Alherz, A.; Musgrave, C. B.; Glusac, K. D., Thermodynamic and kinetic hydricities of metal-free hydrides. *Chem. Soc. Rev.* **2018**, *47* (8), 2809-2836.
- 127. Bonin, J.; Maurin, A.; Robert, M., Molecular catalysis of the electrochemical and photochemical reduction of CO₂ with Fe and Co metal based complexes. Recent advances. *Coord. Chem. Rev.* **2017**, *334*, 184-198.
- 128. Costentin, C.; Drouet, S.; Robert, M.; Savéant, J.-M., A Local Proton Source Enhances CO₂ Electroreduction to CO by a Molecular Fe Catalyst. *Science* **2012**, 338 (6103), 90–94.
- 129. Costentin, C.; Robert, M.; Savéant, J.-M., Current Issues in Molecular Catalysis Illustrated by Iron Porphyrins as Catalysts of the CO₂-to-CO Electrochemical Conversion. *Acc. Chem. Res.* **2015**, *48* (12), 2996-3006.
- 130. Walker, B. R.; Manabe, S.; Brusoe, A. T.; Sevov, C. S., Mediator-Enabled Electrocatalysis with Ligandless Copper for Anaerobic Chan–Lam Coupling Reactions. *J. Am. Chem. Soc.* **2021**, *143* (16), 6257-6265.
- 131. Xiong, P.; Hemming, M.; Ivlev, S. I.; Meggers, E., Electrochemical Enantioselective Nucleophilic α -C(sp³)–H Alkenylation of 2-Acyl Imidazoles. *J. Am. Chem. Soc.* **2022**, *144* (15), 6964-6971.
- 132. Kellett, C. W.; Swords, W. B.; Turlington, M. D.; Meyer, G. J.; Berlinguette, C. P., Resolving orbital pathways for intermolecular electron transfer. *Nat. Comm.* **2018**, 9 (1), 4916.
- 133. Md. Ahsan, H.; Breedlove, B. K.; Cosquer, G.; Yamashita, M., Enhancement of electrocatalytic abilities toward CO₂ reduction by tethering redox-active metal complexes to the active site. *Dalton Trans.* **2021,** *50* (38), 13368-13373.
- 134. Singha, A.; Mondal, A.; Nayek, A.; Dey, S. G.; Dey, A., Oxygen Reduction by Iron Porphyrins with Covalently Attached Pendent Phenol and Quinol. *J. Am. Chem. Soc.* **2020**, *142* (52), 21810-21828.
- 135. Mittra, K.; Chatterjee, S.; Samanta, S.; Dey, A., Selective 4e⁻/4H⁺ O₂ Reduction by an Iron(tetraferrocenyl)Porphyrin Complex: From Proton Transfer Followed by Electron Transfer in Organic Solvent to Proton Coupled Electron Transfer in Aqueous Medium. *Inorg. Chem.* **2013**, *52* (24), 14317-14325.
- 136. Samanta, S.; Sengupta, K.; Mittra, K.; Bandyopadhyay, S.; Dey, A., Selective four electron reduction of O_2 by an iron porphyrin electrocatalyst under fast and slow electron fluxes. *ChemComm* **2012**, *48* (61), 7631-7633.

TOC:

